Miocene rifting of Fuerteventura (Canary Islands)

Carlos Fernández,[1] Ramón Casillas,[2] Encarnación García Navarro,[1] Margarita Gutiérrez,[3] Manuel A. Camacho,[1] and Agustina Ahijado[2]

Received 22 December 2005; revised 23 August 2006; accepted 13 September 2006; published 30 November 2006.

[1] The older geological units of the volcanic island of Fuerteventura (Canary Islands), i.e., the so-called basal complex and the lower part of the subaerial volcanic rocks, show abundant structures indicative of a long-lived period of Miocene tectonic activity. These structures include faults, dike swarms, kilometer-scale folds, tilted sequences, and fissural and central volcanic edifices. A detailed structural study, based on geological mapping and the use of fault slip inversion techniques and statistical analysis of dike orientation, has allowed the identification of three separated Miocene deformation phases: M-D_1, M-D_2, and M-D_3. The average extension directions determined for these phases are NW-SE, NNE-SSW, and ENE-WSW, respectively. A model of oceanic lithosphere rifting is proposed to account for this deformation history. A buoyant, anomalous sublithosphere mantle triggered the extension in the lithosphere beneath Fuerteventura, isolating it during the early and middle Miocene from the plate-scale collision regime predominant in the NW corner of the African plate. **Citation:** Fernández, C., R. Casillas, E. García Navarro, M. Gutiérrez, M. A. Camacho, and A. Ahijado (2006), Miocene rifting of Fuerteventura (Canary Islands), *Tectonics*, *25*, TC6005, doi:10.1029/2005TC001941.

1. Introduction

[2] Volcanic edifices in oceanic intraplate islands have been extensively studied during the last decades due to both academic and economic interests. Volcanic islands mostly lie above hot spots and their analysis is essential to test alternative models on how the lithosphere and the sublithosphere mantle contribute to the kinematics and dynamics of plates [e.g., *Foulger et al.*, 2005]. Active volcanoes are highly dynamical structures with intervening episodes of growth and structural failure [e.g., *McGuire et al.*, 1996]. Understanding this complex evolution is the best tool for risk mitigation and to guarantee safety of populations. Modern research is focused in the study of the relationships between regional and local stress fields, and geometrical, kinematic and rheological evolution of volcanic edifices and their substratum. Methodology includes numerical and analogue modeling [e.g., *van Wyk de Vries and Matela*, 1998; *Cecchi et al.*, 2005] and field studies [e.g., *van Wyk de Vries et al.*, 2001]. A considerable effort has been recently devoted to the analysis of the role of regional tectonics on the evolution of oceanic islands. Apart from the cases of obvious association of oceanic volcanoes with diverging plate boundaries (Iceland, Azores) [e.g., *Searle*, 1980; *Bull et al.*, 2003], a lively debate is going on about the origin of oceanic intraplate islands and island chains as a result of plume- or nonplume-related magmatism (interesting material on this topic can be found at http://www.mantleplumes.org/). Unfortunately, very few works have addressed the problem of analyzing deformation structures in a regionally stressed shield-volcano substratum. This is the main goal of this contribution, devoted to the study of the structures associated with the growth of the large Miocene shield volcanoes in the Fuerteventura Island (Canary Archipelago).

[3] The Canary Islands are a volcanic archipelago located at the eastern Atlantic Ocean, not far from the NW Africa coast. Several hypotheses concerning the origin of the Canary Islands have been presented. These include the mantle plume hypothesis [*Morgan*, 1971; *Holik et al.*, 1991; *Hoernle and Schmincke*, 1993; *Hoernle et al.*, 1995; *Carracedo et al.*, 1998], the propagating fracture hypothesis [*Anguita and Hernán*, 1975], the local extensional ridge [*Fúster*, 1975], and the uplifted tectonic blocks [*Araña and Ortiz*, 1991]. Unfortunately, most of these models have been elaborated with a scarce knowledge of the main structural features and tectonic evolution of the archipelago. This lack of structural information is especially important for the lower units that, in the Fuerteventura Island, include the uplifted oceanic crust, the rocks of the submarine stage of growth, and the plutonic roots of the subaerial volcanic successions. Significant advances have been made in the last years, and an increasing number of structural data have been gathered in the distinct islands of the archipelago [e.g., *Casillas et al.*, 1994; *Marinoni and Pasquarè*, 1994; *Fernández et al.*, 1997; *Marinoni and Gudmundsson*, 2000; *Fernández et al.*, 2002]. The structural evolution of the Lanzarote Island (Figure 1, inset) has been polyphasic, as shown by *Marinoni and Pasquarè* [1994] for the posterosional evolution stage of that island. *Marinoni and Pasquarè* [1994] recognized at least two recent (<6 Ma) deformation phases that generated predominantly strike-slip faults, a tectonic regime that fits the predictions of numerical models for the northwestern African plate [*Jiménez-Munt and Negredo*, 2003]. Ductile-

[1]Departamento de Geodinámica y Paleontología, Universidad de Huelva, Huelva, Spain.
[2]Departamento de Edafología y Geología, Universidad de La Laguna, La Laguna, Tenerife, Canary Islands, Spain.
[3]Estudios del Terreno S.L., Santa Úrsula, Santa Cruz de Tenerife, Canary Islands, Spain.

0278-7407/06/2005TC001941

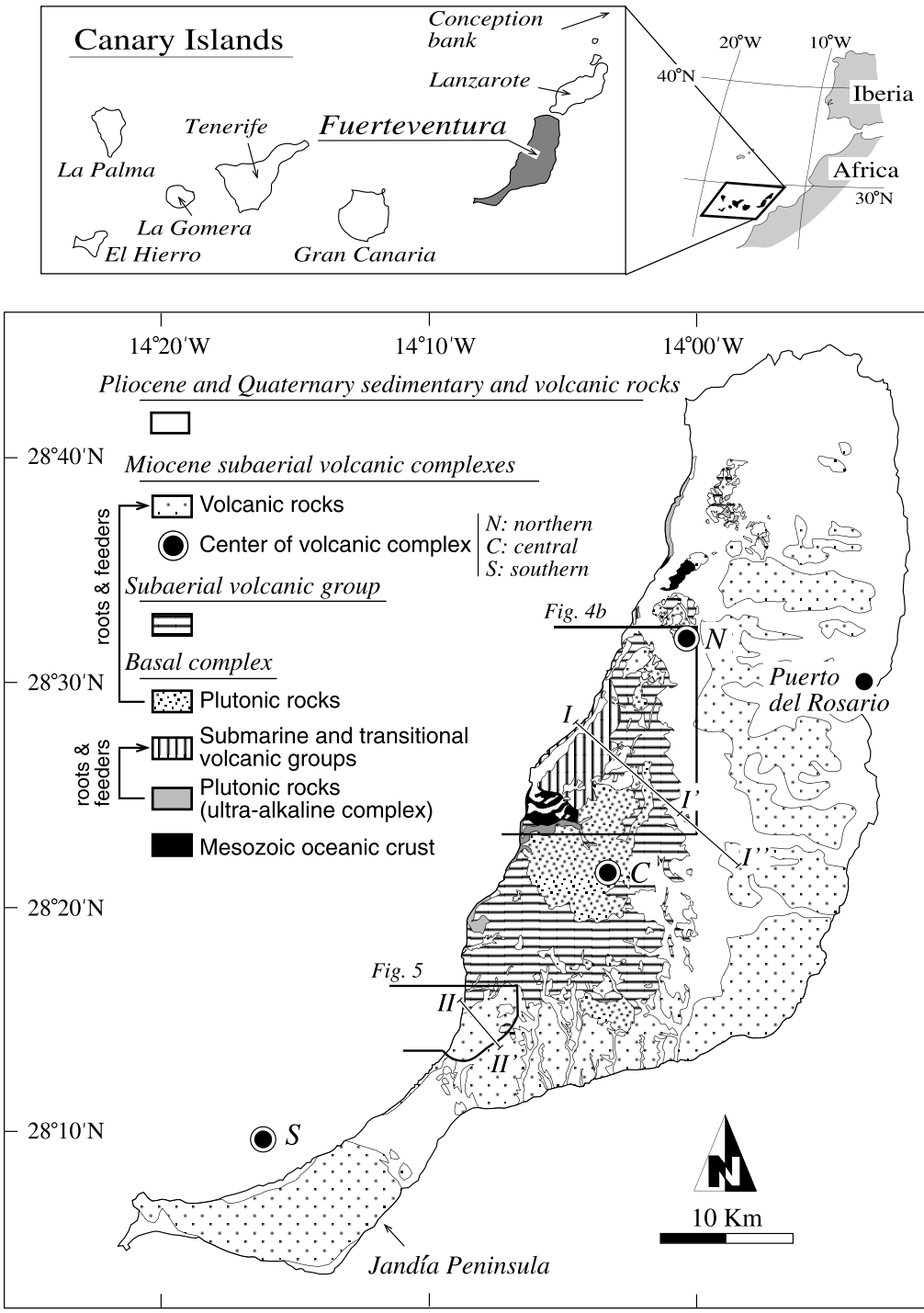

Figure 1. Location of the Fuerteventura Island in the Canary Archipelago and simplified geological map of the island. Modified from *Ancochea et al.* [1993]. The outlined areas correspond to the regions mapped in detail and shown in Figures 4b and 5. Cross sections I-I′-I″ and II-II′ are also shown. S, C and N refer to the centers of the large volcanoes described by *Ancochea et al.* [1993].

brittle shear zones have been described in Fuerteventura [*Casillas et al.*, 1994; *Fernández et al.*, 1997]. These shear zones generated during an old extensional episode (~25 Ma), contemporary with the transition from submarine to subaerial growth of Fuerteventura [*Gutiérrez et al.*, 2006]. Polyphase brittle deformations have also been described for the shield-building stage of Tenerife (<8 to >3 Ma) [*Marinoni and Gudmundsson*, 2000] and La Palma (<2 Ma) [*Fernández et al.*, 2002]. However, the structural information is scarce and irregularly distributed

across the archipelago, and much more work remains to be done in this field. These data are fundamental to any comprehensive model attempting to explain the origin of the Canary Islands.

[4] New information concerning the Miocene tectonic evolution of the Fuerteventura Island is presented in this work. The Oligocene tectonic history of Fuerteventura, coeval with its submarine stage of growth, has been presented elsewhere [*Gutiérrez*, 2000; *Gutiérrez et al.*, 2006]. This work is primarily focused on the study of the Miocene deformation stages, which coincided with the main episodes of the subaerial volcanic evolution of the island. Section 5 includes some ideas about the implications of the results of this work to unravel the tectonic origin of the archipelago, and to contribute to the understanding of the structural evolution of some volcanic edifices in oceanic islands associated with hot spots. Current discussion on plumes, plates and magmatism [e.g., *Foulger et al.*, 2005] can also benefit from the results of this work.

2. Geological Setting

[5] Fuerteventura is located at the eastern Canary ridge [*Coello et al.*, 1992], defined by a NNE-SSW trending volcanic province comprising the Fuerteventura and Lanzarote Islands, and their submerged prolongation at the Conception Bank [*Weigel et al.*, 1978; *Dañobeitia*, 1988] (Figure 1). The geological history of Fuerteventura is long and complex [*Fúster et al.*, 1968; *Stillman et al.*, 1975; *Fúster et al.*, 1980; *Le Bas et al.*, 1986; *Sagredo et al.*, 1989; *Coello et al.*, 1992; *Ancochea et al.*, 1996; *Steiner et al.*, 1998; *Balogh et al.*, 1999; *Muñoz et al.*, 2005], and the island lies on the Atlantic oceanic crust, Early Jurassic in age [*Banda et al.*, 1981; *Steiner et al.*, 1998]. Depth to the Moho beneath Fuerteventura is of 15–20 km [e.g., *Dañobeitia and Canales*, 2000]. A layer 2–4 km thick with seismic velocities of 4.2–4.3 km s^{-1} characterizes the upper crust. This layer overlies the middle crust, with a thickness of 5–6 km and seismic velocities of 6.1–6.6 km s^{-1}. Finally, the basal part of the crust coincides with a 7.4 km s^{-1} velocity layer, 8–10 km thick, interpreted as oceanic crust intruded by mantle-derived material [*Watts*, 1994]. The upper mantle shows seismic velocities of 7.6–7.8 km s^{-1} above Fuerteventura [*Dañobeitia and Canales*, 2000].

[6] For the purposes of this work, four main units can be distinguished in the island (Figure 1). These are, from mostly older to younger, the basal complex [*Fúster et al.*, 1968; *Stillman et al.*, 1975], the subaerial volcanic group [*Gutiérrez*, 2000], the Miocene subaerial volcanic complexes, and the Pliocene and Quaternary sedimentary and volcanic rocks. These units are described with detail in this section previous to the analysis of their structural characteristics.

2.1. Basal Complex

[7] In this work, the basal complex includes the exposures of the Mesozoic oceanic crust, the submarine and transitional volcanic groups, and the plutonic bodies and dike swarms associated with these groups and with the subaerial volcanic units. Former studies considered the subaerial volcanic group as a part of the basal complex [e.g., *Fúster et al.*, 1968; *Stillman et al.*, 1975]. However, the work of *Gutiérrez* [2000] has shown the distinctive characteristics of this subaerial group and, given its tectonic relevance, it has been distinguished here from the basal complex.

[8] The outcropping fragment of Mesozoic oceanic crust consists of a thick sedimentary sequence (around 1600 m) overlying tholeiitic normal mid-ocean ridge basalts [*Robertson and Stillman*, 1979a; *Robertson and Bernouilli*, 1982; *Steiner et al.*, 1998]. The terrigenous and pelagic sedimentary succession spans from the Early Jurassic to the Late Cretaceous [*Steiner et al.*, 1998], and it was deposited at a deep-sea fan derived from the West African continental margin [*Fúster et al.*, 1968; *Robertson and Stillman*, 1979a; *Robertson and Bernouilli*, 1982; *Steiner et al.*, 1998].

[9] Resting unconformably on the Mesozoic oceanic crust is the submarine volcanic group [*Robertson and Stillman*, 1979b; *Fúster et al.*, 1984a, 1984b; *Le Bas et al.*, 1986; *Stillman*, 1987, 1999; *Gutiérrez*, 2000; *Gutiérrez et al.*, 2006]. This unit is composed of primary volcanic facies and volcanogenic facies (nomenclature after *McPhie et al.* [1993]), which are characterized by the presence of rocks with ultra-alkaline affinity and strongly alkaline rocks. The age of the submarine volcanic group is Oligocene, and it has been interpreted as a syntectonic unit with respect to a NNE-SSW directed extension [*Gutiérrez*, 2000; *Gutiérrez et al.*, 2006].

[10] Onlapping the submarine volcanic group is the transitional volcanic group. This is a lithostratigraphic unit, late Oligocene in age, which has been interpreted as a result of explosive plinian subaerial eruptions, lava deltas, shallow water effusive eruptions, gravity flows, and shallow water reefs [*Gutiérrez*, 2000; *Gutiérrez et al.*, 2006]. Late during the deposition of the transitional volcanic group started the ESE-WNW directed extensional episode characterizing the Neogene subaerial building of the island, whose study is the main objective of this contribution.

[11] Plutonic and hypabyssal rocks, probably associated with the submarine and transitional volcanic groups, form the ultra-alkaline complex [*Fúster et al.*, 1980; *Le Bas et al.*, 1986; *Ahijado and Hernández-Pacheco*, 1990; *Muñoz et al.*, 2005]. The younger of these rocks became emplaced contemporary with displacement along brittle and ductile extensional shear zones [*Casillas et al.*, 1994; *Fernández et al.*, 1997]. These zones were active during the late Oligocene, around 25 Myr ago [*Le Bas et al.*, 1986; *Cantagrel et al.*, 1993; *Sagredo et al.*, 1996; *Ahijado*, 1999; *Balogh et al.*, 1999], therefore heralding the Neogene extensional episodes that are described in this work.

[12] A cortege of plutonic rocks (pyroxenites, gabbros and syenites) and a dike swarm crosscut the whole of the previously described units in the basal complex [*Gastesi*, 1969, *Muñoz*, 1969] as well as the rocks of the subaerial volcanic group. These rocks are mostly Miocene, and they have been interpreted as the hypabyssal roots of the successive episodes of growth of the subaerial volcanic edifices [*Ancochea et al.*, 1996; *Balogh et al.*, 1999; *Muñoz et al.*, 2005].

2.2. Subaerial Volcanic Group

[13] The subaerial volcanic group rests unconformably on the units forming the basal complex (Figure 1). A very heterogeneous unit of basalts, trachybasalts, debris-avalanche breccias and debris-flow breccias form this group, which is intensely crosscut by the previously mentioned basic dikes and plutons. The density of the dike swarm has obliterated many of the original features of these rocks, although lava flows, sometimes of pahoehoe type, and their related autoclastic breccias are commonly observed. This group has been originally defined by *Gutiérrez* [2000], who first described its subaerial character, thus separating it from the clearly submarine and transitional rocks of the basal complex. The age of this group has not been determined, but it must be comprised between the last stages of deposition of the transitional volcanic group [23 Ma after *Gutiérrez*, 2000] and the oldest episodes of the Miocene subaerial volcanic complexes (20–22 Ma according to *Ancochea et al.* [1996]).

[14] The rocks forming the basal complex and the subaerial volcanic group suffered a locally intense hydrothermal metamorphism of greenschist facies. The origin of this metamorphism is the massive intrusion of dike swarms and plutons related to the subaerial volcanic rocks [*Fúster et al.*, 1968; *Stillman et al.*, 1975; *Robertson and Stillman*, 1979b; *Fúster et al.*, 1984a; *Javoy et al.*, 1986; *Muñoz and Sagredo*, 1994; *Hobson et al.*, 1998; *Gutiérrez*, 2000].

2.3. Miocene Subaerial Volcanic Complexes

[15] Three huge basaltic volcanic constructs were generated during the Miocene in Fuerteventura: the southern, central, and northern edifices (Figure 1) [*Ancochea et al.*, 1996]. The growth of each edifice was punctuated by periods of volcanic quiescence associated with erosion and development of giant landslides [*Ancochea et al.*, 1996; *Stillman*, 1999]. The southern edifice (the SVC of *Ancochea et al.* [1996]) crops out in the Jandía Peninsula (Figure 1), and it was built by three successive constructive episodes, SVC-I, SVC-II, and SVC-III. The bottom of the series (SVC-I, 20.7–19.3 Ma [*Ancochea et al.*, 1996]) is mostly composed of pahoehoe basaltic lava flows, hydromagmatic pyroclasts and quartz-trachytic plugs and tuffs. Locally, resting unconformably on this pahoehoe unit is a level of polymictic breccias, of variable thickness, that is covered by a series of ankaramite lava flows. The SVC-II episode (17.2–15.4 Ma [*Ancochea et al.*, 1996]), formed by lava flows and pyroclasts of basaltic and trachybasaltic composition, lies unconformably above the SVC-I, filling an important paleorelief [*Ancochea et al.*, 1996]. Finally, ankaramite flows, olivine-pyroxene basalts and, to a lesser extent, trachybasalt flows of the SVC-III episode (15.2–14.2 Ma [*Ancochea et al.*, 1996]) lie indistinctly above SVC-I or SVC-II. On the basis of structural and topographic criteria, *Ancochea et al.* [1996] proposed the existence of a large central volcano for SVC-II and SVC-III, with its center located offshore, to the north of the Jandía Península (Figure 1).

[16] Three constructive episodes have been distinguished in the central volcanic complex (the CVC) according to *Ancochea et al.* [1996]. The CVC-I presents a lower unit of polymictic breccias that rest above the lava flows of the subaerial volcanic group. These breccias probably represent debris-avalanche deposits related to gravity slides of unknown dimensions, and they could be correlated with those appearing at the top of the SVC-I. In that case, the subaerial volcanic group and the pahoehoe lavas of the basal SVC-I could correspond to the same volcanic episode. Above the polymictic breccias there appears a thick (>1000 m) sequence of basaltic, mainly ankaramitic, flows, tilted and crosscut by abundant dikes, that will be studied with detail in this work. Thin basaltic flows and pyroclast levels, as well as trachyte flows, plugs and dikes, constitute the CVC-II (22.5–20 Ma [*Ancochea et al.*, 1996]). A polymictic breccia seals the unconformity between CVC-I and CVC-II. Thick flows of basalt and trachybasalt of the CVC-III episode (15.6–14.5 Ma [*Ancochea et al.*, 1996]) lie above CVC-I, CVC-II, or even above the subaerial volcanic group. Again, a central volcanic edifice has been deduced for the CVC (center in Figure 1), with different centers depending on the considered constructive episode.

[17] The northern edifice (NVC) includes two constructive episodes (NVC-I and NVC-II) separated by a volcanic agglomerate unit (Ampuyenta Formation) witnessing the collapse of the NVC-I edifice. Basalts, picritic basalts, oceanitic basalts, trachybasalts and trachytes predominate in NVC-I (22(?)–15.3 Ma [*Ancochea et al.*, 1996]). Basaltic lava flows constitute the NVC-II episode (14.3–12.8 Ma [*Ancochea et al.*, 1996]) that rests unconformably on the Ampuyenta Formation. The available data suggest a central volcanic edifice for NVC-II whose focus has been located at the northern half of Fuerteventura (Figure 1).

[18] It cannot be excluded that a part of the exposure of the subaerial volcanic group, especially the top of this unit in areas densely traversed by dikes, could correspond to rocks of the CVC-I and NVC-I episodes.

2.4. Pliocene and Quaternary Sedimentary and Volcanic Rocks

[19] A period of quiescence followed the Miocene subaerial volcanic activity, and the edifices were deeply eroded. Small basaltic volcanoes and associated lava fields resulted from a renewed activity during the Pliocene that has continued up to prehistoric times. Littoral and shallow water marine deposits, eolian and alluvial complexes and paleosoil deposits were generated in the Pliocene and Quaternary [*Meco and Stearns*, 1981; *Meco and Pomel*, 1985; *Zazo et al.*, 2002].

3. Structural Description

[20] The extensional deformation events that started in the late Oligocene left a structural imprint in the materials of the basal complex, the subaerial volcanic group and the Miocene subaerial volcanic complexes. Three types of structures are studied in this work: dikes, folds and faults.

[21] A dense dike swarm crops out in the western half of Fuerteventura (Figures 2a–2c), essentially affecting the basal complex and the subaerial volcanic group. The impressive spectacle of this dike swarm has attired the attention of a large number of authors [*Fúster et al.*, 1968; *López Ruiz*, 1970; *Stillman and Robertson*, 1977; *Stillman*, 1987; *Ahijado*, 1999; *Ahijado et al.*, 2001]. The composition of these dikes is mainly basaltic or trachybasaltic, though trachyte and phonolite dikes are also found. The emplacement of this dike swarm should have involved a large crustal stretch [*López Ruiz*, 1970; *Stillman and Robertson*, 1977; *Stillman*, 1987; *Ahijado et al.*, 2001]. Measurement of dike orientation in this work has included data of almost 3000 dikes (see section 4). Field analysis of the observed systematic crosscut relationships (Figures 2b and 2c) at each measurement site allows proposing separation into three main dike systems. We have labeled them as system 1, 2 and 3. Dikes of system 1 crosscut the basal complex, the subaerial volcanic group, and the rocks of the lower episode (I) of the Miocene volcanic edifices. Around an 82% of the measured dikes correspond to system 1, and probably more if relative volume proportions were considered (Figure 2b). Dikes of system 2 also affect the rocks of the intermediate episode (II) of the large Miocene volcanoes. Finally, dikes of system 3 also crosscut the rocks of the most recent episode (III) of the Miocene volcanic edifices. A more detailed analysis of dikes, taking into account their kinematic implications, will be done in section 4. Here, only the main features of the geometrical arrangement of dikes will be described. The trends of the distinct dike systems are NE-SW, E-W, and NNW-SSE for systems 1, 2, and 3, respectively (Figure 3), with significant local variations that will be presented and discussed in sections 3 and 4. It must be indicated that these average trends are essentially obtained from dike measurement in the basal complex, the subaerial volcanic group and the lower part of the Miocene subaerial edifices. More complex, radial patterns have been described by *Ancochea et al.* [1996] for dikes of our systems 2 and 3, based on their study of the middle and upper sequences of the Miocene edifices. Instead, our work is focused on the more constant trends shown by dikes in the substratum to these large edifices.

[22] The most relevant geometric feature of system 1 dikes is the spatial arrangement of their average dip senses (Figure 3a). Although the dikes show in general steep dip angles (around 92% of the measured dikes exceed 70°, a value that is similar for the three dike systems), systematic spatial patterns with large areas of constant dip sense can be observed for the dikes of system 1. This feature is illustrated in Figure 3a, which show the statistical average orientation at each site (for a location of the measurement sites, see section 4). Of particular relevance here is the indication of dip sense. In sites with steeply dipping dikes, sampling hazards and measurement errors yield rather erratic average dip direction. Therefore, to show truly representative dip direction results, Figure 3a depicts exclusively the orientation of system 1 dikes in measurement sites with average dips of less than 80°, which is considered as a reasonable limit to exclude the effects of sampling and measurement error. Predominantly east dipping system 1 dikes characterize the central and northern western coast of Fuerteventura. Instead, the central and southern part of the island shows west dipping system 1 dikes with only local deviations. Accordingly, lines marking the change between both dip senses can be traced that represent vertical axial surfaces of large fans defined by downward or upward converging dikes (Figure 3a). By contrast, no systematic spatial arrangement of dip senses can be observed for the dikes of systems 2 and 3 (Figures 3b and 3c). The geometry of the dike density contours will be described below.

[23] Most of the subaerial volcanic rocks and several units of the basal complex show well-defined bedding, of volcanic or sedimentary origin (Figures 2d, 2e, and 2f). The bedding appears partially transposed in zones of high dike density, although it is often possible to measure its trend and dip. Figure 4a shows a summary of the bedding attitude measurements in the submarine, transitional and subaerial volcanic groups, and in the successions of the older constructive episodes of the northern and central volcanic complexes. The most striking feature of this map, apart from the predominant NE-SW trending directions, is the presence of large-scale folds affecting the bedding surfaces. An anticline can be observed in the northwestern part of the island. A close-up view of this structure, which affects the submarine, transitional and subaerial volcanic groups, reveals that it is an open fold, slightly west vergent (Figure 4b). The statistical axis of this fold dips 14° toward the NNE. The dikes of system 1 are mostly normal to the bedding. However, the axial surface of the anticline is not strictly coincident with the surface marking the change in dip sense of dikes (Figure 4b, cross section I-I′). Other folds appear to the east of the anticline, including an open syncline that coincides with the location of the plutonic rocks associated with the Miocene volcanic complexes (Figure 4b).

[24] Steep dipping bedding can be observed at the southern part of the exposure of the basal complex and the subaerial volcanic group (Figures 2d and 4a). This zone (Las Hermosas area) is a part of the eastern limb of the anticline described before in the central part of the island. Detailed mapping of this zone shows a close geometrical association between variations in the bedding dip and a system of NE-SW trending normal faults (Figure 5). The system 1 dikes in this zone are consistently normal to the bedding (Figure 5, cross section II-II′, and Figure 6), and subparallel to the main NW dipping normal faults. Assuming that changes in the bedding dip are related to major curvatures in the fault surfaces, and applying the constant heave Chevron construction [*Williams and Vann*, 1987], a basal detachment can be obtained for the Las Hermosas and La Pared faults (Figure 5, map and cross section II-II′). The cross section is parallel to the average slip sense on the fault surfaces (e.g., Figure 6 and fault data in section 4). The main faults in Las Hermosas area converge toward this basal detachment, which shows a gentle dip to the NW. This hypothetical basal detachment lies at a depth of around 2.5 km below the present-day surface. Other faults can be

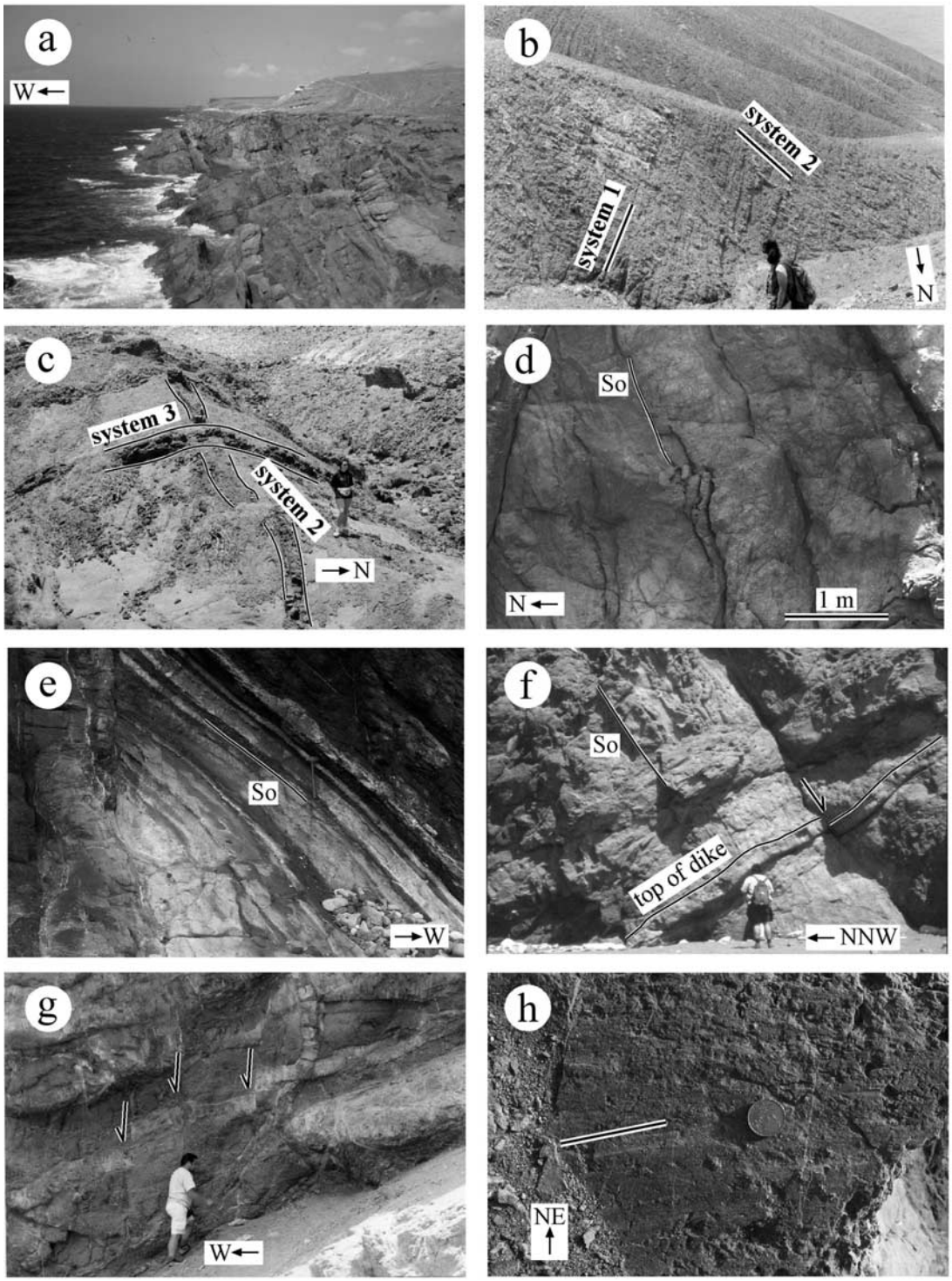

Figure 2. (a) View of the dike swarm that cuts the basal complex in the western coast of Fuerteventura. (b) Dike swarm in the basal complex; dike density larger than 90%. Dikes of system 2 (WNW-ESE) crosscut dikes of system 1 (NNE-SSW). (c) Crosscut relationship between a dike of system 3 (N-S) and a dike of system 2 (E-W) in the Jandía Peninsula. (d) Subvertical bedding shown by the subaerial volcanic rocks in the southwestern coast (Las Hermosas area). (e) Moderately dipping bedding of the submarine volcanic rocks (central western coast of Fuerteventura). (f) Normal fault displacing dikes in the southwestern coast (Las Hermosas area). (g) Normal faults displacing subhorizontal dikes in the west coast, to the north of Las Hermosas area. (h) Slickenside striation (continuous line) in a fault plane affecting the subaerial volcanic group (southwestern coast, Las Hermosas area).

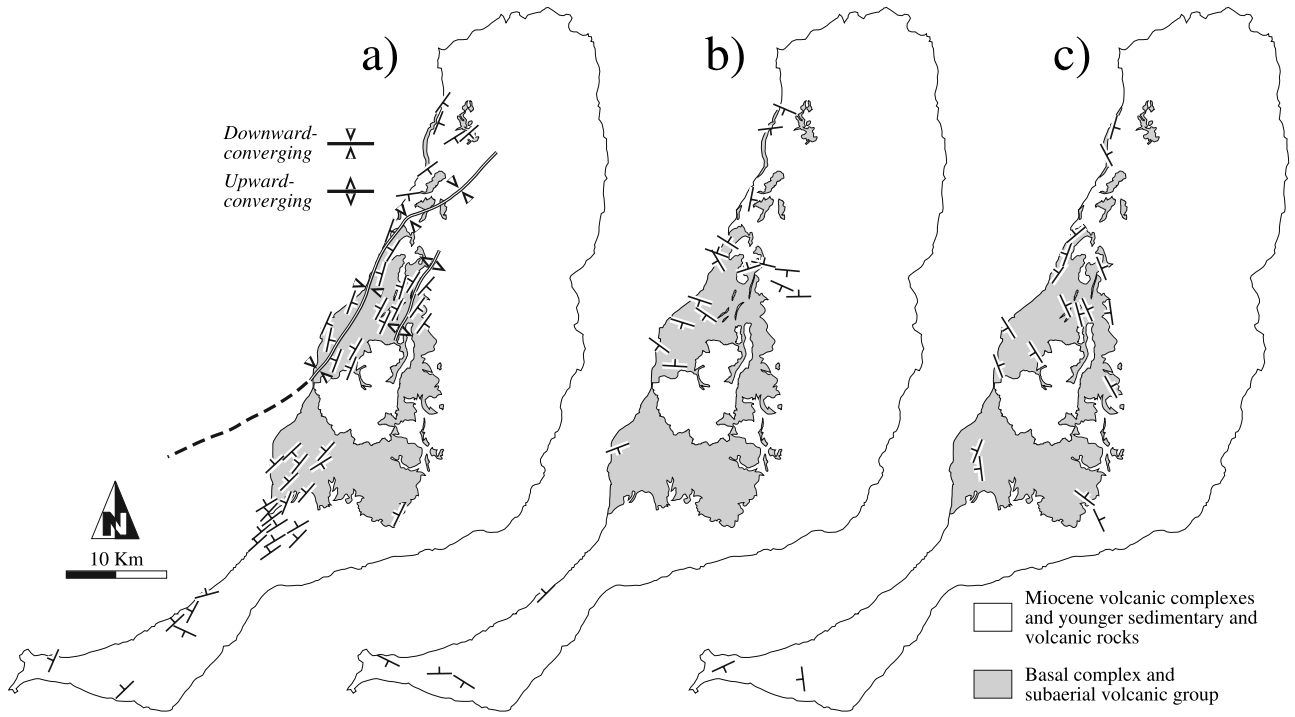

Figure 3. Average orientation (trend and dip direction) of dikes traversing the basal complex, the subaerial volcanic group and the basal episodes of the Miocene volcanic complexes. Only sites with average dips lower than 80° are represented. (a) Dikes of system 1. The traces of the surface with downward converging or upward converging dikes are shown. (b) Dikes of system 2. (c) Dikes of system 3. See text for further explanation.

observed to the SE of Las Hermosas fault, suggesting that the basal detachment must continue in that direction.

[25] The structural data presented in this work are summarized in Figure 7. The axial traces of the bedding folds are parallel and almost coincident with the traces of the axial surfaces to the dike fans (Figure 7a). The traces of these large structures are not straight and two main curvatures can be observed. The NNE-SSW trends predominant in the central area pass to NE-SW trends to the north. The Atlantic Ocean covers the prolongation of these structures to the south, but the NE-SW trends observed in Las Hermosas area seem to indicate that a similar curvature exists in the southern half of the island. Therefore the described structures delineate a huge sigmoid at the scale of the Fuerteventura Island.

[26] Significantly, the density peaks of system 1 dike swarm closely fit the geometry of the sigmoid structures defined by dike and bedding orientation (Figures 7b and 7c). The dike density map nearly coincides with that presented by *Stillman* [1987] in the basal complex. Density of system 1 dikes is partly dependent on the age of their host rocks. Generally speaking, the rocks of the Mesozoic crust show dike densities larger than the subaerial volcanic group, which is contemporary with these dikes (Figure 7c). However, dike densities larger than 90% have been found in rocks ranging in age from the Mesozoic to the Miocene (Figure 7c). On the other side, densities between 20% and 30% are also observed in the Mesozoic oceanic crust. Therefore it must be concluded that dike density is also structurally controlled, with elongate, NNE-SSE to NE-SW trending areas of high dike densities bounded laterally by low dike density bands (Figure 7c). Planimetry of the dike density map (Figure 7b) reveals that the elongation (change in length/initial length) in the studied area is of 0.7–1.0 (70–100%) due to dike intrusion. This large value of elongation is heterogeneously distributed, ranging from 3 at cross section I-I′-I″, to less than 0.5 at cross section II-II′ (location of cross sections in Figure 1). The extension within cross section I-I′-I″ yields a net crustal lengthening of 8 km. Dike densities in the Jandía Peninsula have not been represented in Figure 7 because they are noticeably lower than in the north, rarely exceeding 10%.

4. Kinematic Analysis of Faults and Dikes

[27] A detailed analysis of the structures indicative of brittle deformation has been performed in Fuerteventura to obtain a better understanding of the Miocene tectonic evolution of this island. This study includes inversion of fault slip data and statistical analysis of dike orientation. The data have been obtained in the field, in different measurement sites covering the exposures of the basal complex and Miocene rocks (Figure 8). The rocks of the constructive episodes II and III of the three distinct Miocene volcanic complexes are virtually devoid of faults with reliable kinematic indicators. Accordingly, the sites of fault

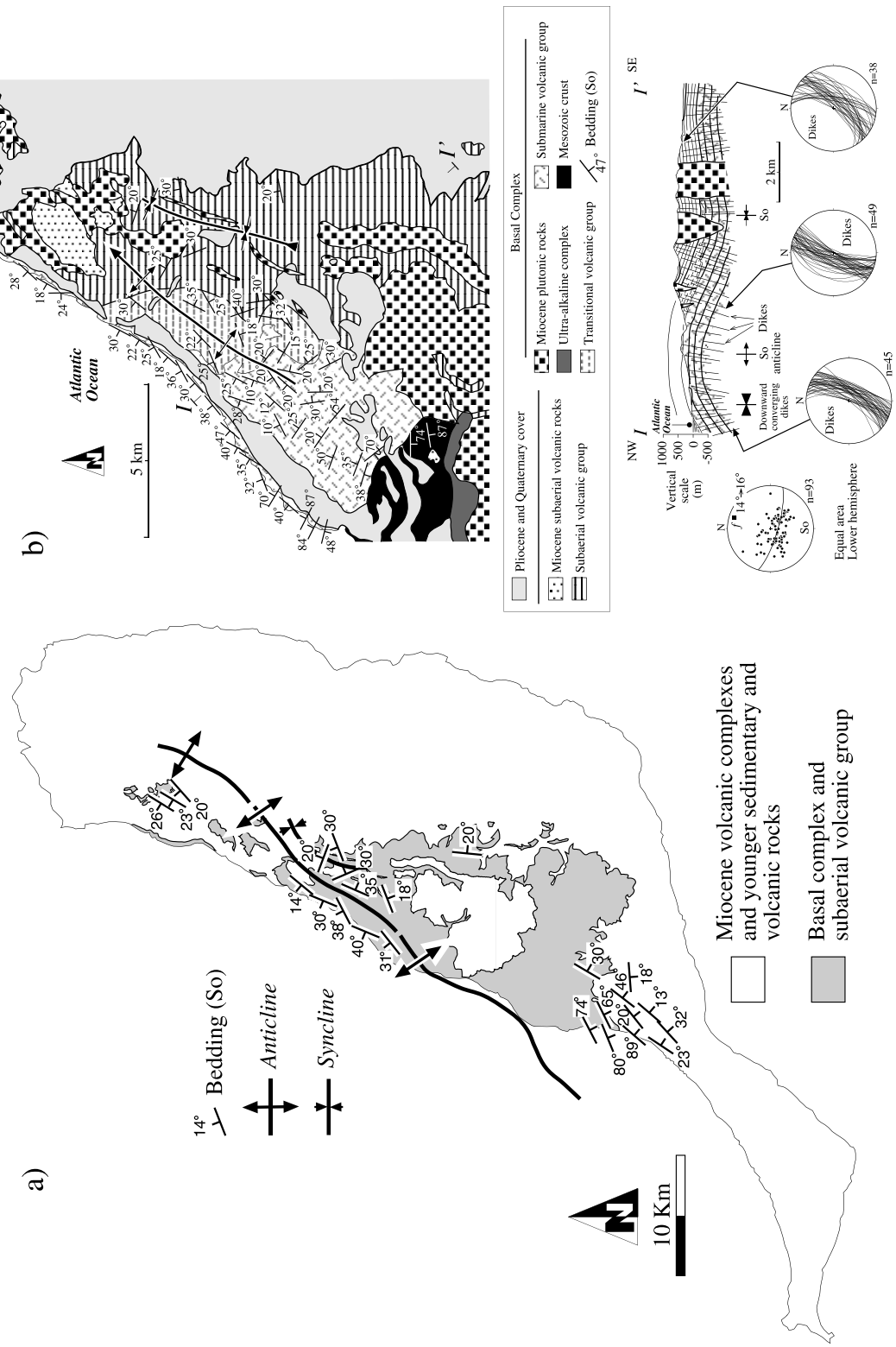

Figure 4. (a) Spatial variation of the bedding orientation in the submarine, transitional, and volcanic groups and in the basal episodes of the Miocene volcanic complexes. A large anticline can be traced near the western coast of Fuerteventura. (b) Detailed geological map of the submarine, transitional, and subaerial volcanic group in central west Fuerteventura (for a location, see Figure 1). The cross section I-I′ shows the main structures. The stereograms show the variation in the dike dip along the cross section, and the poles to the bedding (So) with location of the statistical best fit fold axis (f).

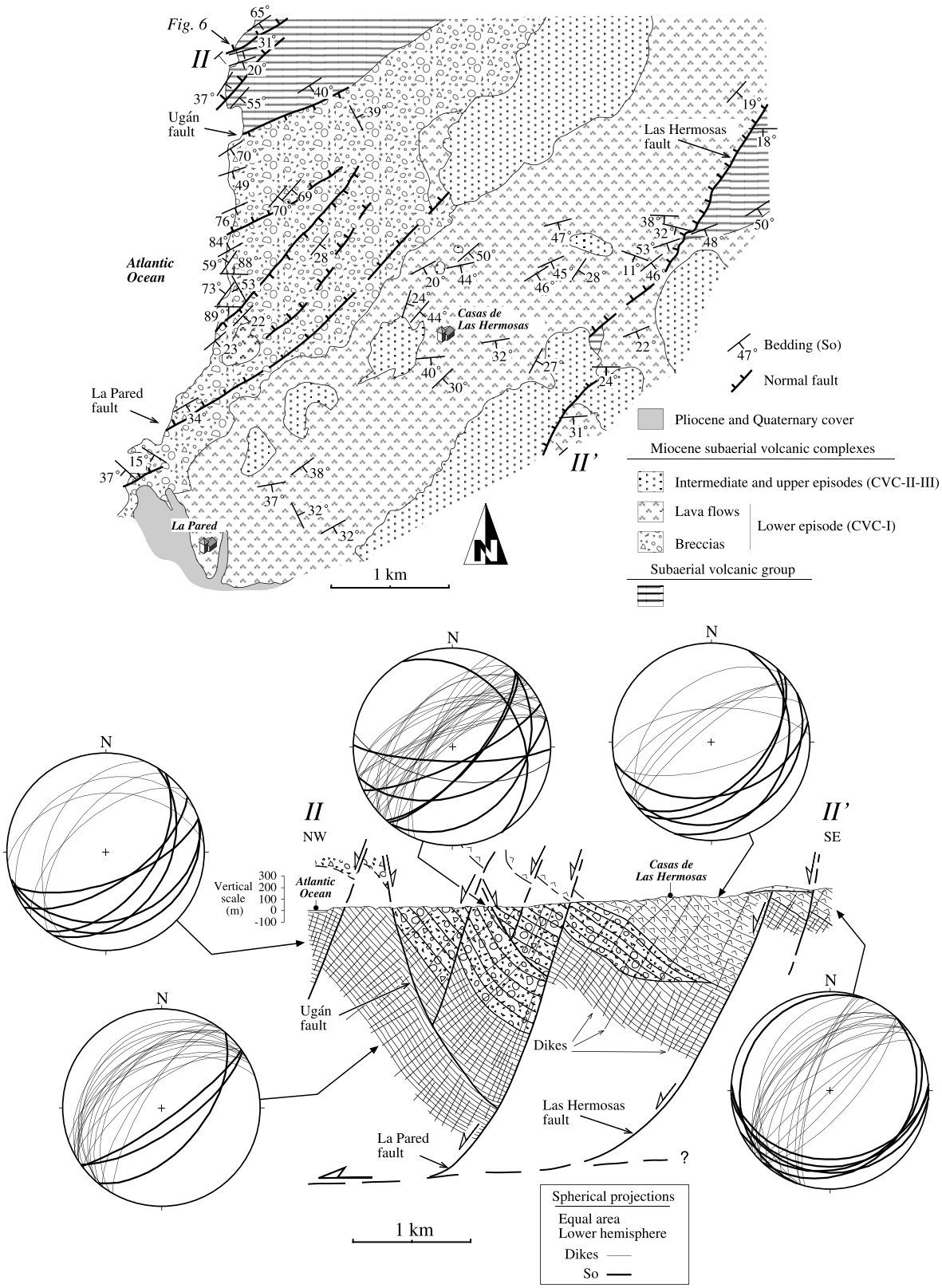

Figure 5. Detailed geological map of the Las Hermosas area (for a location, see Figure 1). Cross section II-II′ shows the reconstruction of the fault geometry at depth. The stereograms include data from bedding (So) and dike orientations. Note the statistically normal arrangement of both types of structures and the distinct tilting angle distinguishable at each block.

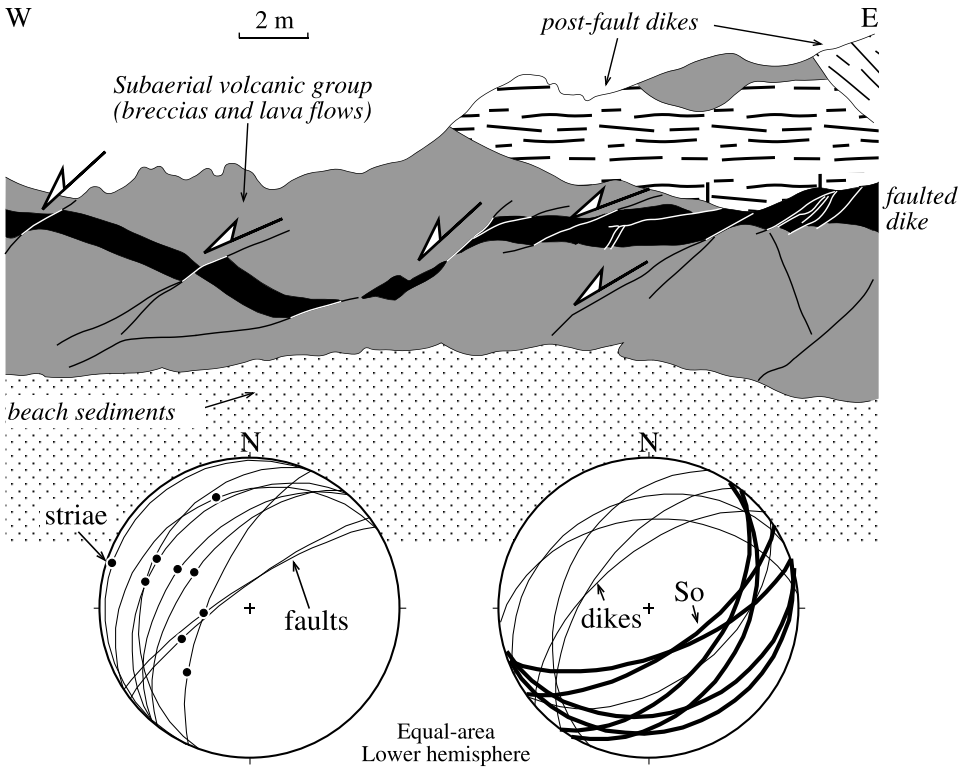

Figure 6. Detailed geometry of the system 1 normal faults displacing subhorizontal dikes in the western coast of Las Hermosas area, near the point II of cross section II-II′ (see Figure 5 for location).

slip measurement are concentrated in the rocks of the basal complex, the subaerial volcanic group and the episode I of the Miocene volcanic complexes. Most of the dike measurement sites are also located in these same rock units, and therefore the discussion of the dike results will also consider the data of the younger episodes (II and III) of the Miocene volcanism given by other authors [e.g., *Ancochea et al.*, 1996].

4.1. Methodology

[28] Fault slip data have been observed in 55 sites (Figure 8a and Table 1) adding together 1780 measured faults. Typically, each data consists of trend, dip and dip sense of the fault surface, pitch of the slickenside striation (Figure 2h), and sense of displacement along the fault. The kinematic analysis of the distinct fault systems has followed the method of *Marret and Allmendinger* [1990]. This is a graphical technique that allows estimating the orientation of the P (infinitesimal principal shortening) and T (infinitesimal principal extension) axes of the incremental deformation tensor for each fault. Once determined the P and T axes for the totality of faults of a given system, the tensor summation for this system is achieved by computing the orientation tensor of these kinematic axes (for a definition of the orientation tensor, see *Scheidegger* [1965] and *Mardia* [1972]). The eigenvectors of the orientation tensor give the orientation of the P and T axes for the entire fault system at each site.

[29] The study of dike orientation includes 2996 measurements of trend, dip and dip sense of dikes determined in 96 sites (Figure 8b and Table 2). Assuming that dikes were generated as fractures of mode I [*Lawn and Wilshaw*, 1975; *Pollard and Segall*, 1987], the maximum extension direction must lie normal to their boundaries [*Walker*, 1987; *Marinoni*, 2001]. As explained before, three dike systems have been distinguished according to the relative crosscutting relationships among them (Figures 2b and 2c). Again, the orientation tensor has been calculated for each system and site. The eigenvector associated with the largest eigenvalue of this matrix gives the orientation of the principal extension direction.

[30] Finally, maps of trajectories of maximum extension have been traced from the results of the statistical analysis fault and dike data at each site. Tracing of trajectories has used the algorithm of *Lee and Angelier* [1994], which takes into account variations in parameters like data dispersion and local gridding effects.

4.2. Results

[31] The results obtained in the studied area are presented in Tables 1 and 2 and in Figures 9, 10, and 11. Stereograms of faults and dikes and determination of principal deformation axes for selected sites are shown in Figures 9a (left) and 10a. The entire set of stereograms is available in the auxiliary material[1].

[1] Auxiliary materials are available in the HTML. doi:10.1029/2005TC001941.

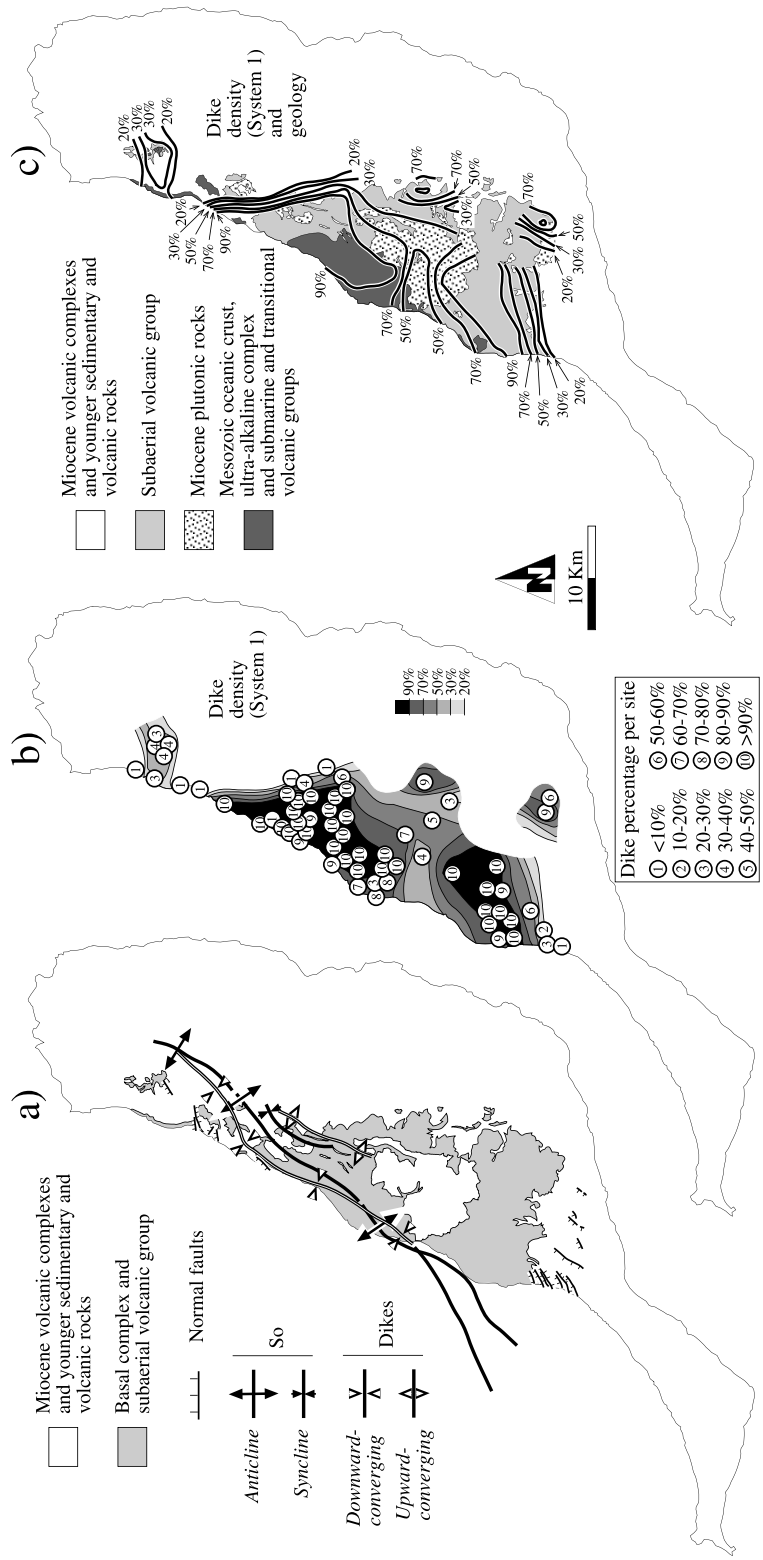

Figure 7. Summary of the main structural data of the basal complex, the subaerial volcanic group and the Miocene volcanic complexes of Fuerteventura. (a) Comparison of the main structures defined from the study of bedding (So) and dike orientation. (b) Dike density contours (system 1) obtained from data of *Gutiérrez* [2000] and this work. At each measurement site the dike percentage has been determined measuring the linear percentage of system 1 dikes versus host rock and excluding younger dikes. (c) Dike density contours (system 1) traced on a geological sketch of Fuerteventura.

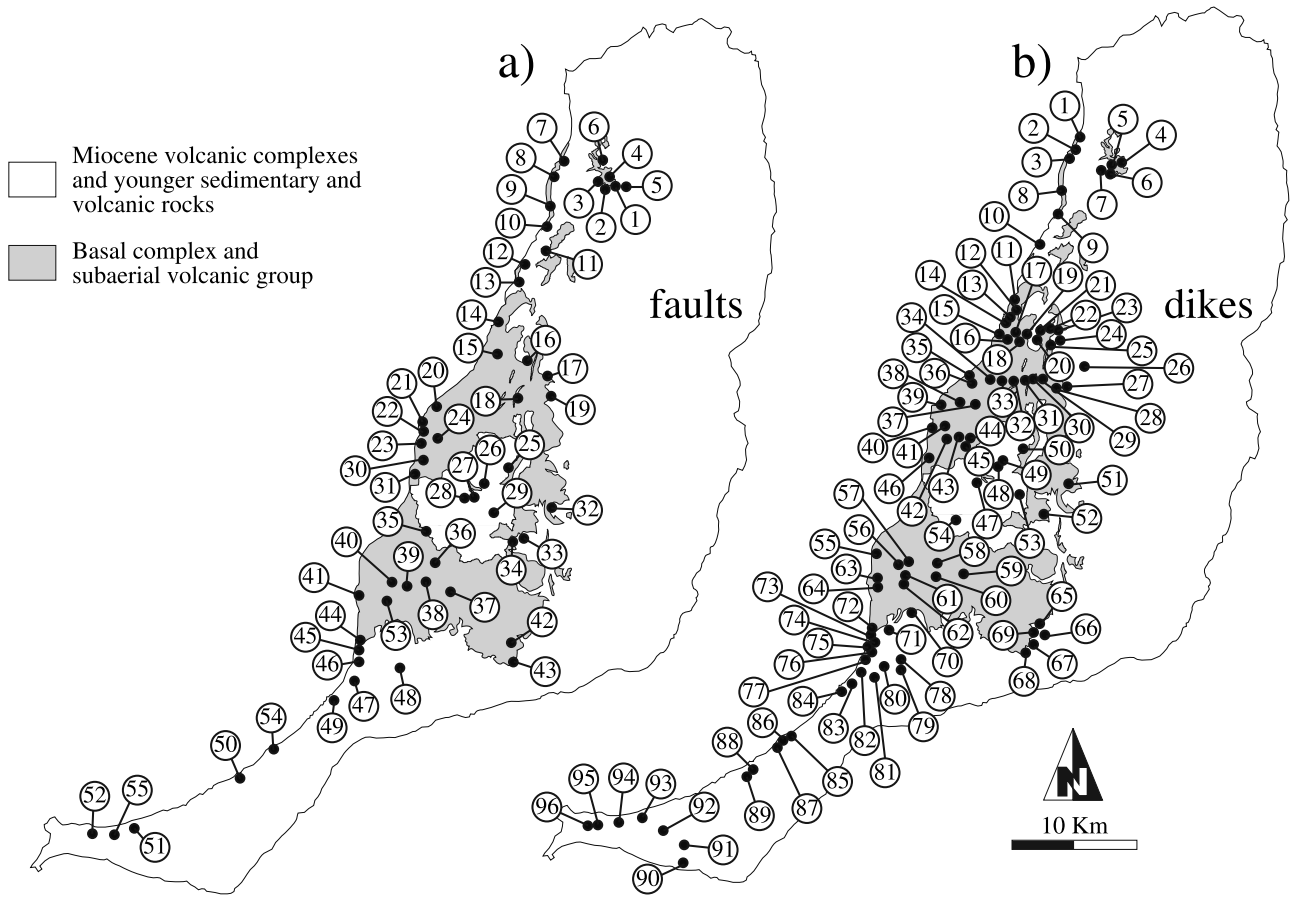

Figure 8. Location of (a) fault, and (b) dike measurement sites. Numbers refer to the sites listed in Tables 1 and 2.

[32] The fault sample obtained at each site has been separated into different systems according to field observations like crosscut relationships and relative age criteria. This technique is probably the most reliable to discriminate among the distinct faulting episodes affecting a given rock volume [*Homberg et al.*, 2004]. In some cases, these discriminating field criteria are not available, and the fault separation has been done by comparison with the results obtained from the study of dikes in the same site or from fault crosscutting in nearby measurement sites. Three fault systems (1, 2, and 3, from older to younger) have been distinguished at the scale of the studied area. System 1 faults are the most abundant, constituting almost a 60% of the measured faults. Systems 2 and 3 represent the 13% and 27% of the measured faults, respectively. All the measured faults are normal (Figures 2f and 2g and Table 1), albeit a strike-slip component is commonly present (Figure 9a). Accordingly, the principal extension axis (T) is subhorizontal in all cases, while P is subvertical (Table 1). The three fault systems distinguished in this work correspond to three distinct tectonic episodes with contrasted orientations of their kinematic axes. The T axes trajectories are NW-SE oriented for fault system 1 (Figures 9b and 11a), although they rotate toward NNW-SSE trends in the Jandía Peninsula. The horizontal extension trajectories for fault system 2 are NNE-SSW oriented, at a high angle, though not normal, to the extension trajectories of fault system 1 (Figures 9b and 11a). Fault system 3 shows E-W extension trajectories. However, NE-SW trends are also common in the northern and southern parts of the island. The trends of the faults of the three systems are statistically normal to those of their corresponding horizontal extension trajectories (Figures 9 and 11a).

[33] The three distinct dike systems (1, 2, and 3, form older to younger) coincide in age and kinematics with the systems defined in the fault study. Also the maps of the horizontal extension trajectories obtained from the dike study (Figure 11b) are very similar to those of faults. Dikes of system 1 are the most abundant. They probably represent more than 90% in volume of the dike swarm, and around 82% of the total number of measured dikes (Table 2). Systems 2 and 3 include the 8% and 10% of the measured dikes, respectively. The dikes in Fuerteventura are mostly subvertical (Figure 10a), although some significant deviations to this rule are important to define the large-scale structure in the basal complex, as explained before. Apart from this, the pole to the average dike boundary, coinciding with the principal extension axis, is subhorizontal in most

Table 1. Results of the Fault Slip Inversion Data Obtained From the Method of *Marret and Allmendinger* [1990][a]

Site	FS	Unit	Nt	P and T Axes (Dip/Strike) P	T
1	1	SaVG	54	79/322	10/128
	3	SaVG	18	86/237	4/51
2	1	SaVG	31	79/337	6/98
	2	SaVG	7	82/141	5/14
3	1	UC	44	67/292	21/132
4	2	UC	15	71/323	13/190
5	1	SaVG	4	77/218	4/111
	2	SaVG	12	80/358	8/212
6	1	UC	38	77/345	6/104
7	1	UC	19	84/242	3/127
	3	UC	5	70/312	6/59
8	3	UC	43	60/330	5/232
9	1	UC	15	74/140	16/318
10	1	UC	13	69/341	19/138
	3	UC	21	75/170	3/70
11	1	MS	34	80/148	10/309
12	3	SmVG	26	79/300	10/95
13	1	SmVG	34	87/94	2/309
14	3	SmVG	9	86/304	4/90
15	1	SmVG	33	83/223	2/115
16	1	SaVG	6	53/59	21/298
17	1	SaVG	23	77/252	11/110
	2	SaVG	17	73/252	8/12
18	1	SaVG	48	67/206	5/104
19	1	SaVG	44	83/258	4/132
20	1	SmVG	19	68/192	12/314
	3	SmVG	19	62/206	10/98
21	3	MS	10	76/131	12/284
22	1	MS	26	86/42	1/295
	2	MS	23	76/28	12/181
23	1	MS	15	69/337	14/107
	2	MS	15	79/351	10/193
24	1	SmVG	16	83/281	7/105
25	2	PS	28	79/147	5/34
26	1	PS	35	87/88	3/290
27	1	PS	8	79/147	11/309
	3	PS	6	20/350	18/87
28	1	PS	7	65/199	8/307
29	2	PS	7	84/172	6/349
	3	PS	33	69/245	17/99
30	2	MS	3	57/208	27/350
	3	MS	41	78/101	11/292
31	1	MS	7	65/248	19/112
	2	MS	3	44/328	20/217
32	3	SaVG	55	71/105	19/278
33	2	SaVG	26	76/7	14/198
	3	SaVG	7	53/3	4/267
34	1	SaVG	23	73/53	4/314
	2	SaVG	12	7/138	2/48
35	1	SaVG	7	81/132	9/315
36	1	SaVG	26	66/122	23/309
37	1	SaVG	51	77/274	11/129
38	3	SaVG	42	72/197	5/93
39	3	SaVG	21	62/170	13/285
40	1	SaVG	25	74/172	11/303
	2	SaVG	7	24/65	4/333
41	1	SaVG	19	76/7	4/113
	2	SaVG	22	83/308	4/178
42	3	UC	52	76/298	11/81
43	3	UC	15	80/67	9/270
44	1	MVS	98	81/256	5/135
45	3	MVS	25	81/31	3/282
46	1	MVS	15	80/320	10/131
47	1	MVS	34	86/277	4/130
48	1	MVS	29	77/102	10/321
	2	MVS	10	78/104	2/205
49	2	MVS	12	76/156	13/353
50	1	MVS	23	81/83	6/309
	3	MVS	25	78/227	12/56
51	1	MVS	44	85/188	5/348
	3	MVS	17	73/238	10/112
52	1	MVS	24	77/87	2/349
53	1	SaVG	42	74/162	13/310
54	2	MVS	13	76/111	1/203
55	1	MVS	23	70/214	16/357

[a]Definitions are FS, fault system; MS, Mesozoic sediments; SmVG, Submarine and transitional volcanic groups; UC, Ultra-alkaline complex; SaVG, Subaerial volcanic group; PS, Miocene plutonic rocks; MVS, Miocene volcanic rocks (episodes SVC-I, CVC-I, and NVC-I); Nt, total number of faults measured and separated in subsets. P and T are kinematic shortening and extension axes.

cases (Table 2). As stated in the structural description, the azimuths of the distinct dike systems are very different (Figures 2b and 2c), therefore suggesting a succession of tectonic stages with contrasted kinematic patterns. Dikes of system 1 bear consistently a NE-SW to NNE-SSW average trend. Contemporary and late to these dikes is the intrusion of banded plutons with alternating bands of pyroxenite and gabbro (Pajara pluton [*Muñoz et al.*, 1997; *Hobson et al.*, 1998]). These alternating bands are NNE-SSW oriented, which coincides with the average trend of system 1 dikes. The map of horizontal extension trajectories for these dikes and plutons shows quite parallel NW-SE trends (Figures 10b and 11b). As in the case of the fault analysis, a change toward a NNW-SSE extension direction can be observed in the Jandía Peninsula. The dikes of system 1 do not affect the episodes II and III of the Miocene volcanic complexes, and are the main responsible for the high dike densities affecting large zones of the basal complex and the subaerial volcanic group (Figures 2a, 2b, 7b, and 7c). The trend of the dikes of system 2 is E-W, with slight variations from NW-SE to NE-SW (Figure 10a). Accordingly, the horizontal extension trajectories are NNE-SSW oriented, although N-S and NNW-SSE trends are observed in the southern part of the island (Figures 10b and 11b). The dikes of system 3 show more variable trends, which rotate from NNW-SSE to NNE-SSW, although even larger variations can be observed in the Jandía Peninsula (Figure 10). Therefore the horizontal extension trajectories obtained for dike system 3 are less constant in strike than for systems 1 and 2 (Figures 10b and 11b). Apart from this variability, an average ENE-WSW trend predominates for system 3.

5. Discussion

[34] The structural data presented in this work are indicative of an extensional tectonic activity affecting Fuerteventura from the end of the Oligocene (25 Ma) to, at least, the middle Miocene (~12 Ma), which is the age of the

Table 2. Fisher Statistical Results of the Dikes Poles[a]

Site	DS	Unit	Nt	t_3 (Dip/Strike)
1	1	UC	11	23/308
	2		3	12/22
2	1	UC	5	16/288
	2		2	6/16
3	2	UC	10	13/353
	3		3	15/286
4	1	MVS	9	3/321
	3		10	9/63
5	1	UC	27	2/317
	3		2	1/259
6	1	MVS	21	10/316
	2		1	0/194
7	1	MVS	22	10/329
	3		1	0/254
8	1	UC	16	4/104
	2		2	8/157
	3		3	28/243
9	1	MS	8	33/322
	3		10	8/109
10	1	SmVG	9	63/352
	2		8	61/282
11	1	SaVG	44	16/289
	2		2	12/212
	3		35	35/137
12	1	SaVG	8	22/119
13	2	SaVG	6	25/200
	3		38	12/112
14	1	SaVG	18	4/298
	2		3	19/55
	3		30	34/122
15	1	SmVG	40	80/106
16	1	SmVG	43	7/299
17	1	SaVG	40	5/96
18	1	SaVG	32	0/100
	2		4	8/194
19	1	SaVG	42	5/93
	2		2	24/163
20	1	SaVG	47	7/300
	2		3	7/191
21	1	SaVG	48	3/302
	2		2	44/193
22	1	SaVG	49	12/107
	3		2	7/62
23	1	SaVG	8	7/129
	3		8	22/247
24	1	SaVG	29	12/121
	2		2	32/4
25	1	SaVG	28	11/313
	2		1	24/29
	3		3	2/72
26	1	MVS	6	9/125
	2		1	29/180
27	1	SaVG	38	16/304
	3		4	18/82
28	1	SaVG	42	12/306
	3		8	2/264
29	1	SaVG	45	4/114
30	1	SaVG	47	14/117
	3		3	15/233
31	1	SaVG	48	11/110
	3		2	22/256
32	1		24	14/120
	3		5	22/245
33	1	SmVG	49	3/115
	2		1	0/170
	3		2	0/235
34	1	SmVG	37	3/298
35	1	SmVG	49	2/115
	2		1	11/33
36	1	SmVG	45	14/291
	2		3	39/18
37	1	SmVG	49	7/109
38	1	SmVG	48	4/292
	2		2	24/14
39	1	SmVG	47	21/296
	2		2	1/195
	3		2	23/57
40	1	MS	46	3/109
	2		2	34/36
41	1	MS	66	15/281
	2		1	7/348
42	1	MS	120	10/107
43	1	SmVG	45	4/116
	2		5	18/183
44	1	SmVG	48	10/120
	2		1	9/170
	3		1	14/60
45	1	MS	13	10/110
	2		3	6/346
46	1	MS	23	6/300
	3		11	18/249
47	1	PS	50	4/129
48	1	PS	21	4/293
	2		14	7/160
	3		14	6/242
49	1	PS	35	1/105
	2		3	17/154
50	1	PS	12	2/106
	2		8	5/345
	3		5	2/64
51	1	SaVG	36	1/128
	2		5	7/352
	3		9	16/242
52	1	SaVG	18	8/120
	2		10	1/158
53	1	PS	17	3/112
	2		1	1/154
	3		7	1/254
54	1	PS	32	10/138
55	2	UC	4	18/340
56	1	SaVG	20	3/317
	3		3	12/111
57	1	SaVG	30	6/131
58	1	SaVG	50	17/130
59	1	SaVG	28	6/123
60	1	SaVG	17	22/325
61	1	SaVG	33	20/128
62	1	SaVG	19	32/134
	3		4	33/89
63	1	SaVG	27	12/136
64	1	SaVG	26	2/154
	3		1	3/99
65	1	SaVG	20	4/125
	3		15	11/217
66	1	MVS	1	20/320
	3		3	12/244
67	1	MVS	24	2/98
68	3	MVS	2	7/218
69	1	UC	20	16/117
70	1	SaVG	16	11/132
71	1	SaVG	12	14/112
72	1	SaVG	4	14/152
73	1	SaVG	9	19/133
74	1	SaVG	28	40/141
75	1	MVS	4	40/137
76	1	MVS	36	17/149
77	1	MVS	2	22/141
78	1	MVS	16	22/150

Table 2. (continued)

Site	DS	Unit	Nt	$\mathbf{t}_3$ (Dip/Strike)
79	1	MVS	2	22/138
80	1	MVS	7	22/151
81	1	MVS	4	24/147
82	1	MVS	38	1/328
83	1	MVS	4	6/138
84	1	MVS	10	7/94
	2		4	5/334
85	1	MVS	12	1/143
86	1	MVS	4	11/165
	2		23	12/134
	3		3	2/33
87	1	MVS	13	12/115
	2		12	8/152
88	1	MVS	78	18/137
	3		2	6/42
89	1	MVS	5	19/21
	2		11	6/1
	3		17	4/277
90	1	MVS	17	20/135
91	2	MVS	5	23/31
	3		1	20/85
92	1	MVS	1	6/300
	2		5	12/41
93	2	MVS	36	9/4
	3		12	3/274
94	1	MVS	3	6/222
	2		15	9/4
	3		10	1/112
95	1	MVS	7	14/112
	2		5	20/29
	3		21	18/347
96	1	MVS	38	1/317

[a]Definitions are DS, dike system; MS, Mesozoic sediments; SmVG, Submarine and transitional volcanic groups; UC, ultra-alkaline complex; SaVG, Subaerial volcanic group; PS, Miocene plutonic rocks; MVS, Miocene volcanic rocks (episodes SVC-I, CVC-I, and NVC-I); Nt, total number of dikes measured and separated in subsets; $\mathbf{t}_3$, eigenvector associated with the least eigenvalue of the orientation matrix [*Scheidegger*, 1965], which coincides with the extension direction.

youngest constructive episodes and dikes of the Miocene volcanic complexes. This tectonic activity followed the previous Oligocene extensional event that was followed by a contractional episode during the late Oligocene [*Gutiérrez et al.*, 2006]. The distinct structures generated during the Miocene events (folds, faults, dikes, plutons, volcanic edifices) show a remarkable geometrical and kinematic coherence. Accordingly, the three defined fault systems can be correlated with the corresponding dike systems, taking into account not only kinematic considerations, but also relative age relationships. Therefore three deformation phases are proposed here, and defined as M-D_1, M-D_2, and M-D_3, to distinguish them from the Oligocene deformation phases (O-D).

5.1. Phase M-D_1

[35] Dikes and faults of system 1 (Figures 3a, 4b, 5, 6, 9, 10, and 11), as well as the large-scale folds of the bedding surfaces (Figure 4) and most of the mapped NE-SW trending faults (Figure 5), affect the same rock units and are assigned to the M-D_1 phase. Dike and fault analysis indicates that an extensional tectonic regime prevailed during M-D_1. The kinematic indicators show a NW-SE to WNW-ESE extension direction (Figures 7a, 9, 10, and 11). A large-scale folding of the crust was developed in this stage, with a sigmoid pattern in plan view (Figure 7a). Most of dikes were intruded during M-D_1, with the areas of higher dike density almost matching the fold culminations or the highly fractured areas (Figures 7b and 7c). The brittle-ductile shear zones described by *Fernández et al.* [1997] affecting the ultra-alkaline complexes show kinematic characteristics identical to those of M-D_1, and it is proposed here that these shear zones represent the early stages of extension associated with the M-D_1 phase. Therefore the inception of the M-D_1 structures can be extended back to 25 Ma (Figure 12). Faults of system 1 affect part of the Miocene plutonic rocks that have been dated at around 20 Ma [*Sagredo et al.*, 1996; *Muñoz et al.*, 1997; *Balogh et al.*, 1999]. Similarly, *Feraud* [1981] and *Feraud et al.* [1985] have dated dikes of system 1, which yielded ages ranging from 20.3 to 19.9 Ma. Therefore it is proposed that the M-D_1 phase lasted from 25 Ma to around 20 Ma. The Mesozoic oceanic crust, the submarine volcanic group, and the older rocks of the ultra-alkaline complexes and of the transitional volcanic group are pretectonic rocks (Figure 12). Instead, the younger rocks of the ultra-alkaline complexes and of the transitional volcanic group, the subaerial volcanic group, a part of the Miocene plutonic rocks, most of the basic dike swarm and the early episodes of the Miocene volcanic complexes are syntectonic with M-D_1 (Figure 12). *Ancochea et al.* [1996] identified several deformation phases according with the distinct unconformities separating the episodes of the Miocene volcanic complexes. The M-D_1 phase approximately coincides with phase F_1 of *Ancochea et al.* [1996].

[36] With respect to the tectonic interpretation of M-D_1, there are several possible explanations of the observed structures. A contractional event could be proposed for the large-scale folding. However, the geometrical association between folds and tilted bedding, dikes and normal faults seems to discard that possibility. Emplacement of magma at depth can induce doming at surface [e.g., *Jackson and Pollard*, 1990] and it can also explain the intrusion of the dike swarm. However, bedding plane reverse faults, and normal and reverse faults at high angle to bedding are predicted to develop at the overburden [*Jackson and Pollard*, 1990]. Furthermore, the geometry of the exposed plutonic rocks in the basal complex (Figures 1 and 4) does not correlate with the shape and location of the large-scale anticline (Figure 4). In particular, most of the mapped plutons coincide with the axial trace of large-scale synclines. Therefore the available geological data dismiss the interpretation of the M-D_1 structures in terms of intrusion-controlled doming. However, this mechanism could have played an active role in the generation of some local structures, like the southern periclinal closure of the syncline mapped in Figure 4b. Concentric flexural folds and thrusts are structures normally developed at the ductile substratum of large volcanoes as a consequence of gravitational spreading [*Merle and Borgia*, 1996; *van Wyk de*

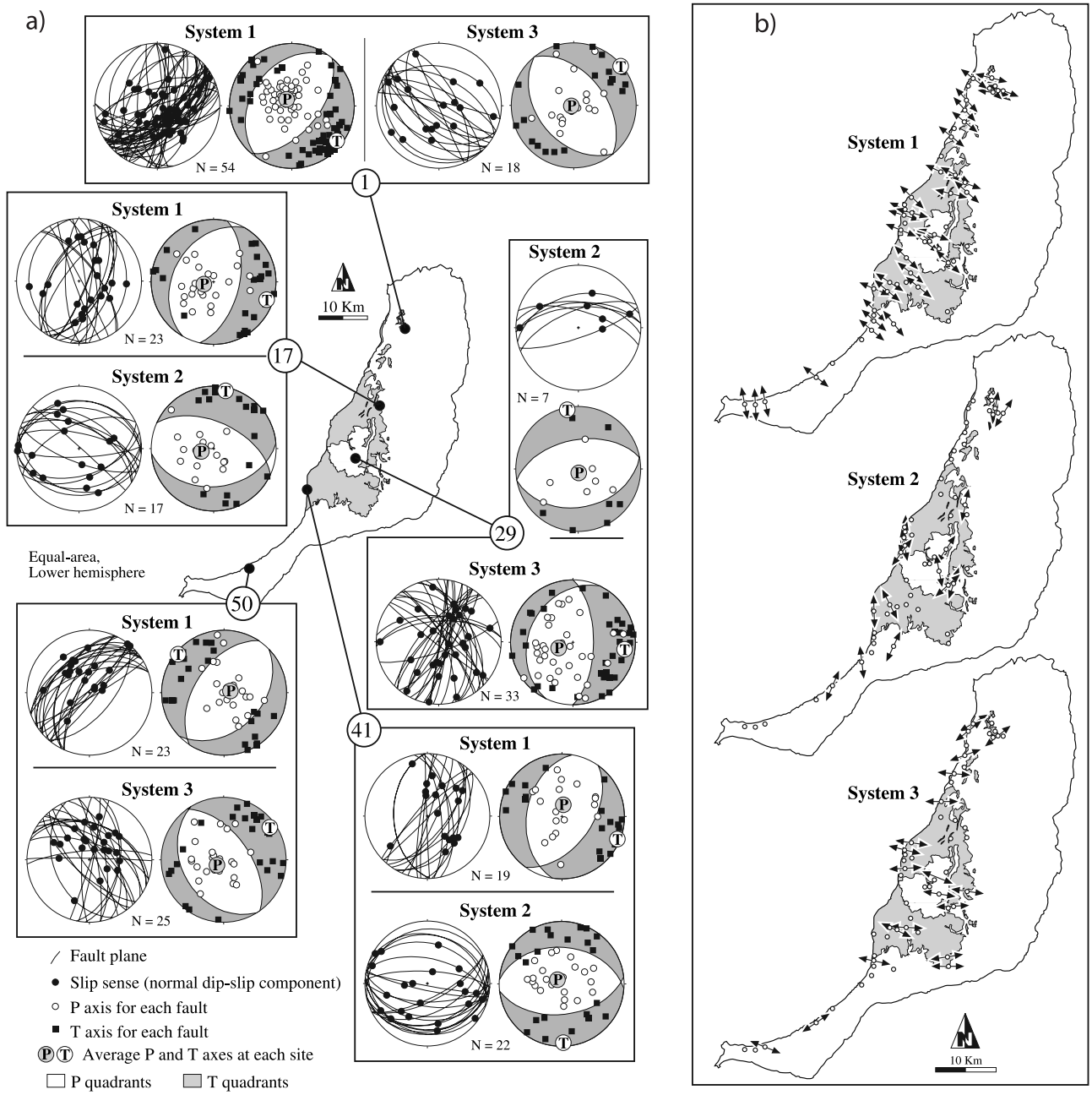

Figure 9. (a) Selected examples of fault measurement sites representing (left/top) great circles of fault planes and slickenside striations; all the faults are normal (black dots) with variable component of strike-slip displacement and (right/bottom) results of the PT method of *Marret and Allmendinger* [1990]. Open circles and solid squares mark the location of the maximum shortening (P) and maximum extension (T) axes for each fault, respectively; the white and gray quadrants represent the regions of the projection with predominance of P and T axes, respectively; the large circles labeled P and T show the location of the average deformation axes for each site and fault system. Numbers refer to the chosen measurement sites located in Figure 8. (b) Spatial distribution of azimuths of the T (maximum extension) axes for fault systems 1, 2, and 3.

Vries et al., 2001; *Oehler et al.*, 2005]. This interpretation faces several problems. First, compressive structures do not normally appear at the base of the volcano, but they are generally located about 20 km from its base [*Oehler et al.*, 2005]. Comparison of our Figures 1 and 4a indicates that the folds are located less than 10 km from the center of the central edifice of Fuerteventura, at a location where numerical models predict subvertical maximum compres-

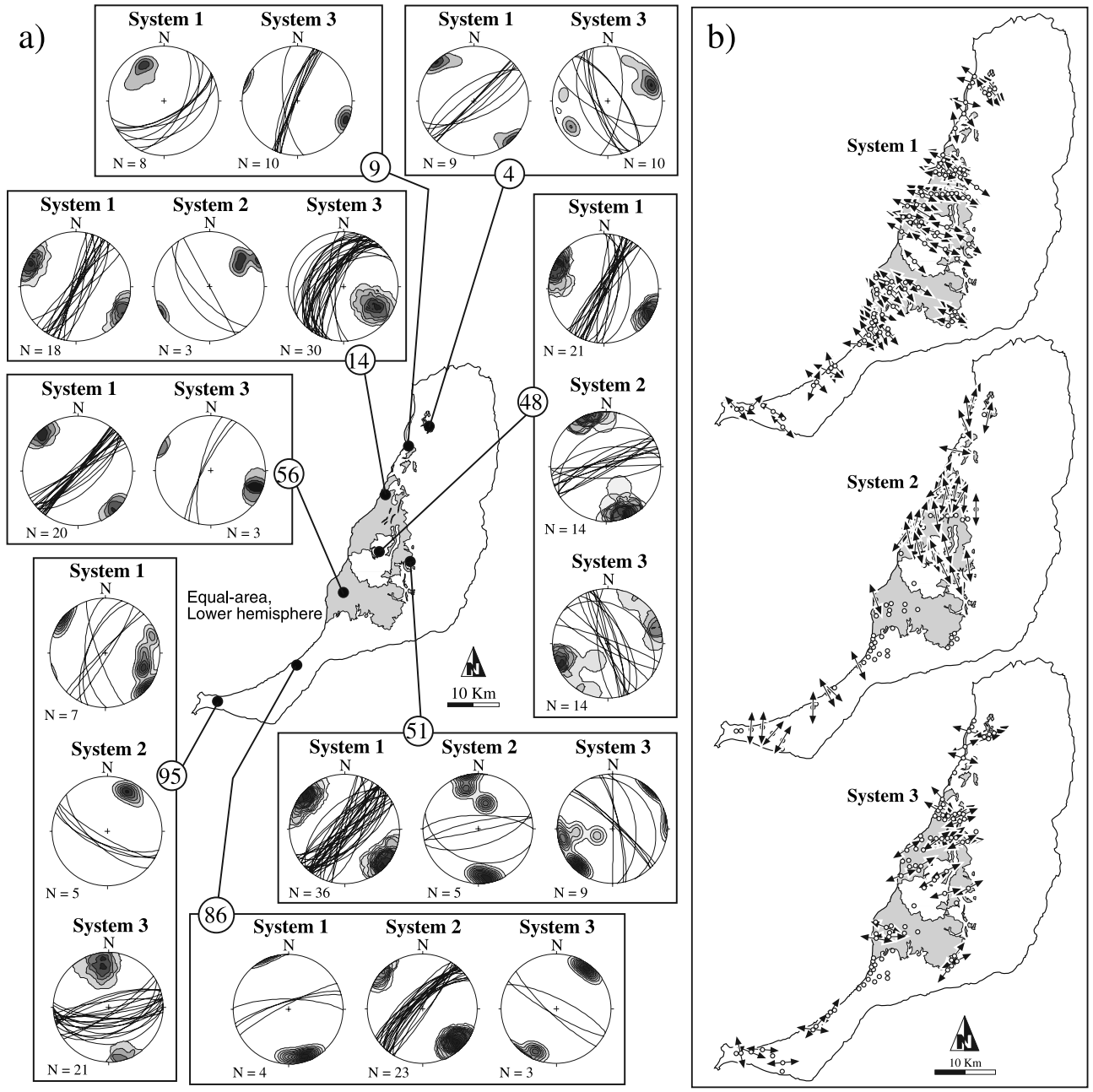

Figure 10. (a) Selected examples of dike measurement sites. The stereograms show cyclographic projections of the measured dikes at each site. Dike separation into systems has been performed by field crosscut relationships. Density contours of the poles to the dikes are also shown. Density diagrams after the *Kamb* [1959] method with the number of expected values under uniform distribution equal to 5 times the standard deviation. Numbers refer to the chosen measurement sites located in Figure 8. (b) Spatial distribution of azimuths of the T (maximum extension) axes for dike systems 1, 2, and 3.

sive stress [*van Wyk de Vries and Matela*, 1998]. Second, the folds described here are associated with normal faults and axial plane parallel dikes, and not with thrusts and strike-slip faults, as is common in extruded substrata to volcanoes [*van Wyk de Vries et al.*, 2001]. Third, the basal complex is mostly composed of lava flows, basic dikes and plutons, ultramafic intrusives and stiff sedimentary rocks. The volcano should have caused a very small deformation field on such a high-viscosity substratum [*van Wyk de Vries and Matela*, 1998], probably not enough to generate the observed structures. Last, the M-D_1 phase was contemporary with the early episodes of the Miocene volcanic complexes, dominated by fissural eruptions. Volcano was probably less than 1000 m high, which again implies small

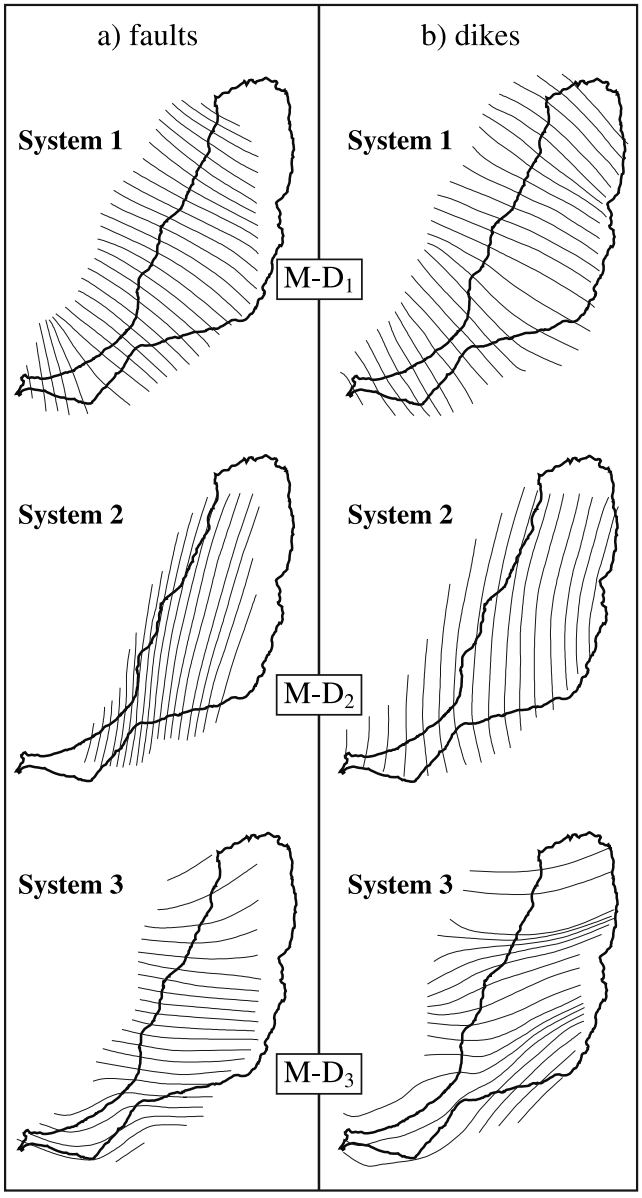

Figure 11. Maps of trajectories of the maximum horizontal extension axis. Results are shown for (a) faults and (b) dikes and are separated according to the distinguished systems (deformation phases M-D_1, M-D_2, and M-D_3). Trajectories obtained from the results of Tables 1 and 2 and using the interpolation program of *Lee and Angelier* [1994].

deformation of its substratum. The final hypothesis considered here for M-D_1 is that of a regional extensional tectonics, modulated by the intrusion of plutons and dikes and by the increasing load of the subaerial volcanic edifices. The structural data presented in this work highly support this hypothesis. However, the precise geometry of the extensional megastructure is debatable, although a possible interpretation is given below.

[37] The geometrical relationships between folds and faults in Las Hermosas area point to the activity during M-D_1 of a linked extensional fault system with a basal detachment slightly dipping to the WNW or NW (cross section II-II′, Figure 5). According to this interpretation, the faults show listric geometry in cross section and the arrangement of the fault system implies an asymmetric WNW to NW directed extension of the crust. Following the same logic, the geometrical analysis of cross section I-I′ (Figure 4b) suggests that the large-scale folds could be associated with a hypothetical basal detachment, that must lie at greater depths in the center of the Fuerteventura Island than in Las Hermosas zone. Cross section I-I′ has been continued until point I″ (Figure 13a; for location, see Figure 1) to obtain more information about the possible location of the hypothetical basal detachment in the center of the island. Cross section I-I′-I″ is based on the surface data and cross section of Figure 4b. The prediction of the geometry of the putative detachment at depth has been obtained by the use of conventional balanced cross section construction techniques and depth to detachment calculations [e.g., *Gibbs*, 1983; *Williams and Vann*, 1987]. Alternation of anticlines and synclines along the cross section has been interpreted as successive rollovers and ramp synclines formed above a complex ramp/flat listric detachment [*McClay and Scott*, 1991] (compare Figures 13a and 13b). The geometry of the subaerial volcanic group is very similar to the theoretical architecture of the synrift sediments in the analogue modeling, while most of the basal complex can be considered as prerift unit (Figure 13a). Also the lower part of the Miocene volcanic complexes can be considered as synrift materials. The converging pattern of system 1 dikes in Fuerteventura (Figure 3a) can be interpreted as a result of emplacement along the fracture system defining the central collapse graben that shows a fan-shaped geometry (Figure 13b). Alternatively, the dikes could have been tilted with respect to the graben axis to become almost parallel to the fan-shaped fault system, like that observed in the Solea graben of Troodos ophiolite [*Allerton and Vine*, 1987]. The association of large folds, dike swarm and normal faults is therefore an essential characteristic of this model. Interestingly, the Miocene plutonic rocks in the cross section I-I′-I″ are located above one of the hypothetical detachment ramps. Moreover, the center of the northern volcanic edifice lies above these plutonic roots (Figure 13a), suggesting a tectonic control on volcanic activity. The breakaway of the basal detachment should be located beneath the lava flows of the upper episodes of the Miocene volcanic complexes (near point I″ in Figure 13a), and it continues to the east of Las Hermosas area, as explained before. The probable trace of the hypothetical breakaway approximately follows the eastern boundary of the central depression of Fuerteventura, a conspicuous morphological feature of the island, although rocks of the episodes II and III of the Miocene volcanic edifices cover the breakaway trace.

[38] The present-day depth to the proposed basal detachment beneath the anticline is of around 5 km. This value, obtained from the techniques used to draw and evaluate cross section I-I′-I″, probably increases to $\geq$6 km below the Atlantic Ocean (left tip of that cross section). Around 2 to 3 km are deduced for the zone to the east of point I′, therefore coinciding with the value in Las Hermosas area

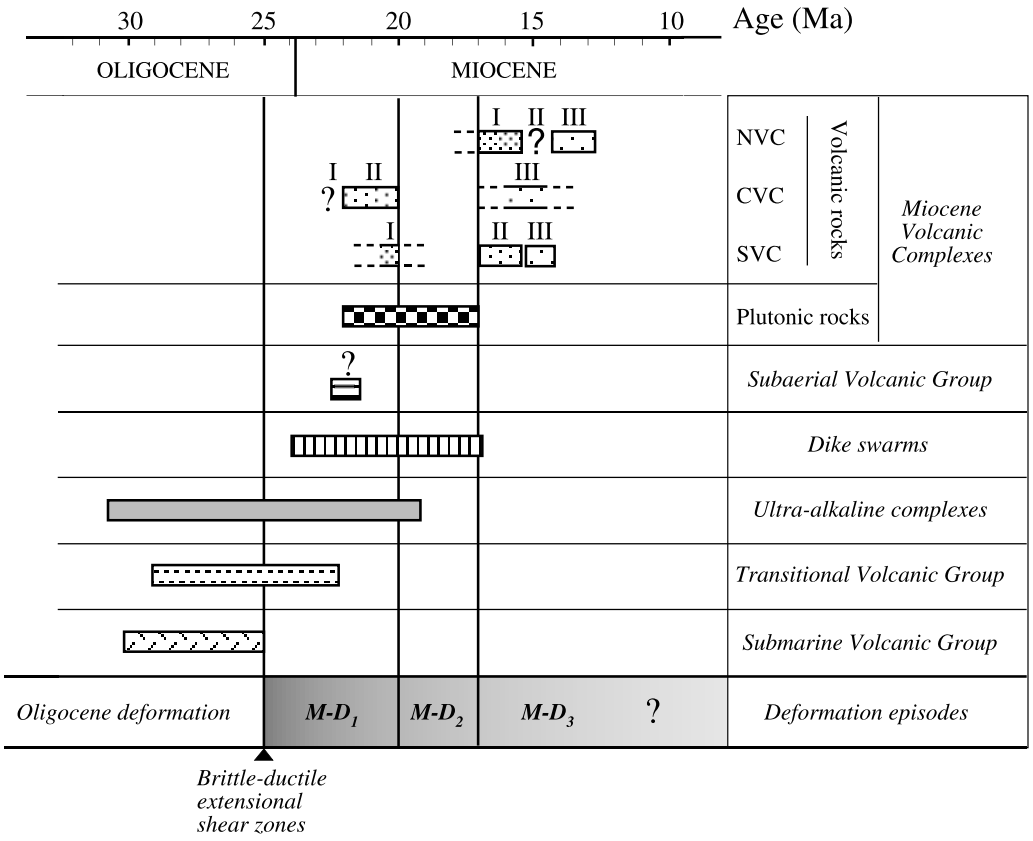

Figure 12. Chronological diagram representing the age of the main units of the basal complex, subaerial volcanic group, and Miocene volcanic complexes of the Fuerteventura Islands (references in the main text). The relative age of the deformation phases distinguished in this work (M-D_1, M-D_2, and M-D_3) is shown for comparison. Age determinations are from *Feraud* [1981], *Feraud et al.* [1985], *Le Bas et al.* [1986], *Ibarrola et al.* [1989], *Cantagrel et al.* [1993], *Ahijado* [1999], *Balogh et al.* [1999], *Gutiérrez* [2000], and *Muñoz et al.* [2005] for the basal complex, the dike swarm and the subaerial volcanic group and *Coello et al.* [1992], *Balcells et al.* [1994], and *Ancochea et al.* [1996] for the Miocene volcanic complexes.

(Figure 5). This is probably due to the vicinity of this zone to the breakaway fault. Figure 14a shows an idealized block diagram depicting the proposed tectonovolcanic activity during the M-D_1 phase. Cross sections I-I′-I″ and II-II′ are shown in the right frontal walls of the block diagram. The thickness of the oceanic crust agrees with the crustal models obtained from seismic profiles [*Banda et al.*, 1981; *Watts*, 1994; *Dañobeitia and Canales*, 2000]. The lower crust in the block diagrams also include a layer with high P wave velocities (7.4 km s^{-1}) found at 14–15 km beneath the surface in Fuerteventura and Lanzarote, and interpreted as due to underplated mafic rocks [*Dañobeitia and Canales*, 2000]. The subaerial volcanic group (and probably the lower units of episode I in the central and southern volcanic complexes) is considered as a synrift unit. The system 1 dike swarm acted as a feeder structure of these volcanic units, and therefore the emission model proposed for these successions consists in an elongate ridge with fissural volcanic activity (Figure 14a). In this sense, the results of this work coincide with the interpretation of *Fúster* [1975] and *Stillman et al.* [1975], at least for the early stages of the subaerial volcanic history of Fuerteventura.

[39] The model of extension favored in this work is asymmetric (Figure 14). The exposed basal complex and subaerial volcanic rocks affected by M-D_1 show predominant east dipping bedding (Figure 4a), and the main mapped faults dip to the west (Figures 5 and 7a). This large-scale architecture recalls that of an asymmetric normal-faulting province (Figure 14). Other arguments are the presence of the central depression to the east of the basal complex exposure, and the distinct geological characteristics of the east and west coasts of Fuerteventura (Figure 1), including the contrasted bathymetry offshore both coasts of the island [e.g., *Acosta et al.*, 2003]. Finally, the giant landslides that partially destroyed the Miocene subaerial shield volcanoes show consistent dips to the west or WNW (Figure 13a), a fact already described by many authors [e.g., *Ancochea et al.*, 1996; *Stillman*, 1999; *Acosta et al.*, 2003]. Recent analogue models suggest that volcano spreading becomes concentrated on downslope sectors even with small (<1°) substrata tilt [*Wooller et al.*, 2004]. Therefore the polarity of

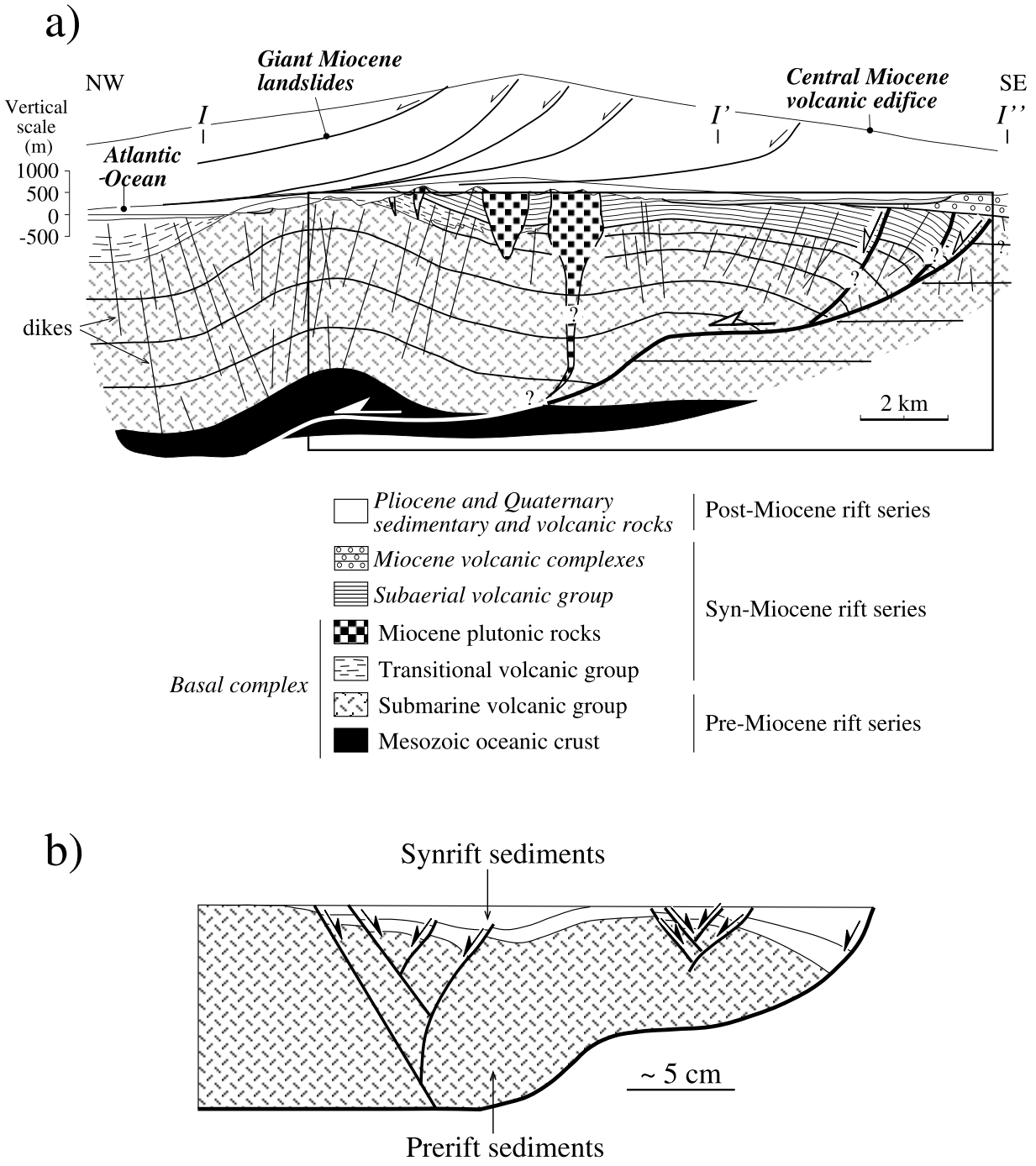

Figure 13. (a) I-I′-I″ cross section (see Figure 1 for location) with interpretation of the geometry and location of a stepped basal detachment. Shape of the large Miocene landslides affecting the volcanic edifice according to *Stillman* [1999]; the rectangle marks the area comparable with the analogue model (Figure 13b). (b) Analogue model of extension above a ramp/flat basal listric detachment (modified after *McClay and Scott* [1991]).

the giant landslides in Fuerteventura can be a consequence of a basement regionally tilted to the west or WNW, which is easy to explain with an asymmetric mode of extension. The absence of accurate geological and geophysical data offshore the west coast of Fuerteventura, does not allow a complete confirmation of the proposed model. Reactivation of the old structures imprinted in the oceanic crust since its birth in the Atlantic ridge, and the influence of younger structures such as the proposed Oligocene detachment [*Gutiérrez et al.*, 2006] have not been evaluated in this work, although these structural inheritances cannot be dis-

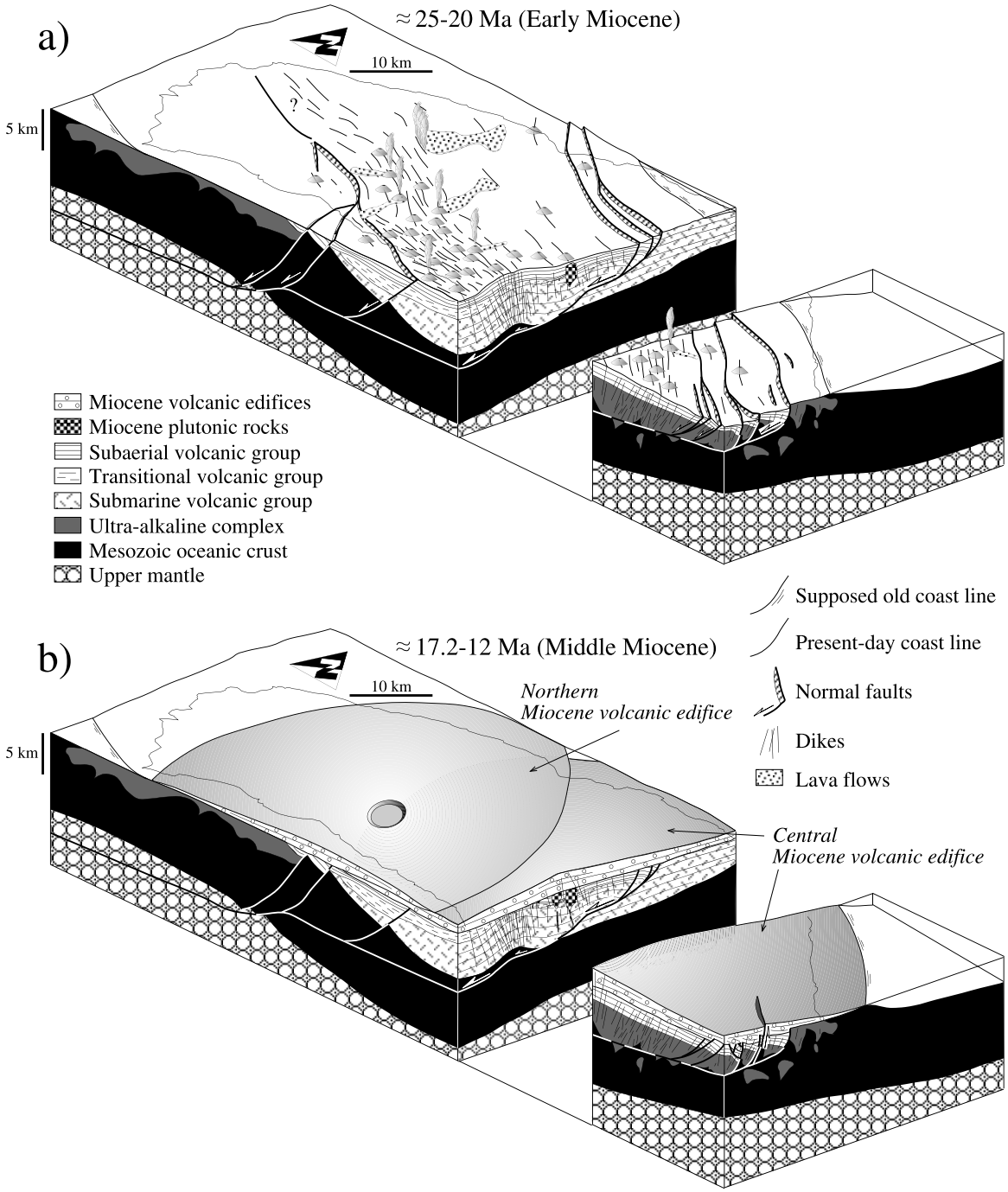

Figure 14. Idealized block diagrams showing the geometry of the structures resulting from the Miocene deformation in the Fuerteventura Island. (a) Reconstruction during the M-D_1 phase depicting the displacement along a basal extensional detachment, the upward arching of the crust and the fissural volcanism generating the subaerial volcanic group. (b) Reconstruction during the M-D_3 phase representing the northern and central Miocene volcanic edifices (approximate size and geometry after *Ancochea et al.* [1993]). The three seismic layers identified in Fuerteventura by *Dañobeitia and Canales* [2000] correspond broadly to the Miocene volcanic edifices (upper crust), the submarine and transitional volcanic groups (middle crust), and the Mesozoic oceanic crust variably intruded by mantle magmas (lower crust). However, exact coincidence cannot be expected, due to the complex three-dimensional architecture of the crust in Fuerteventura. Thinning of the crust toward north is also observed in the seismic profile studied by *Dañobeitia and Canales* [2000]. The present-day coastline of Fuerteventura is shown for reference.

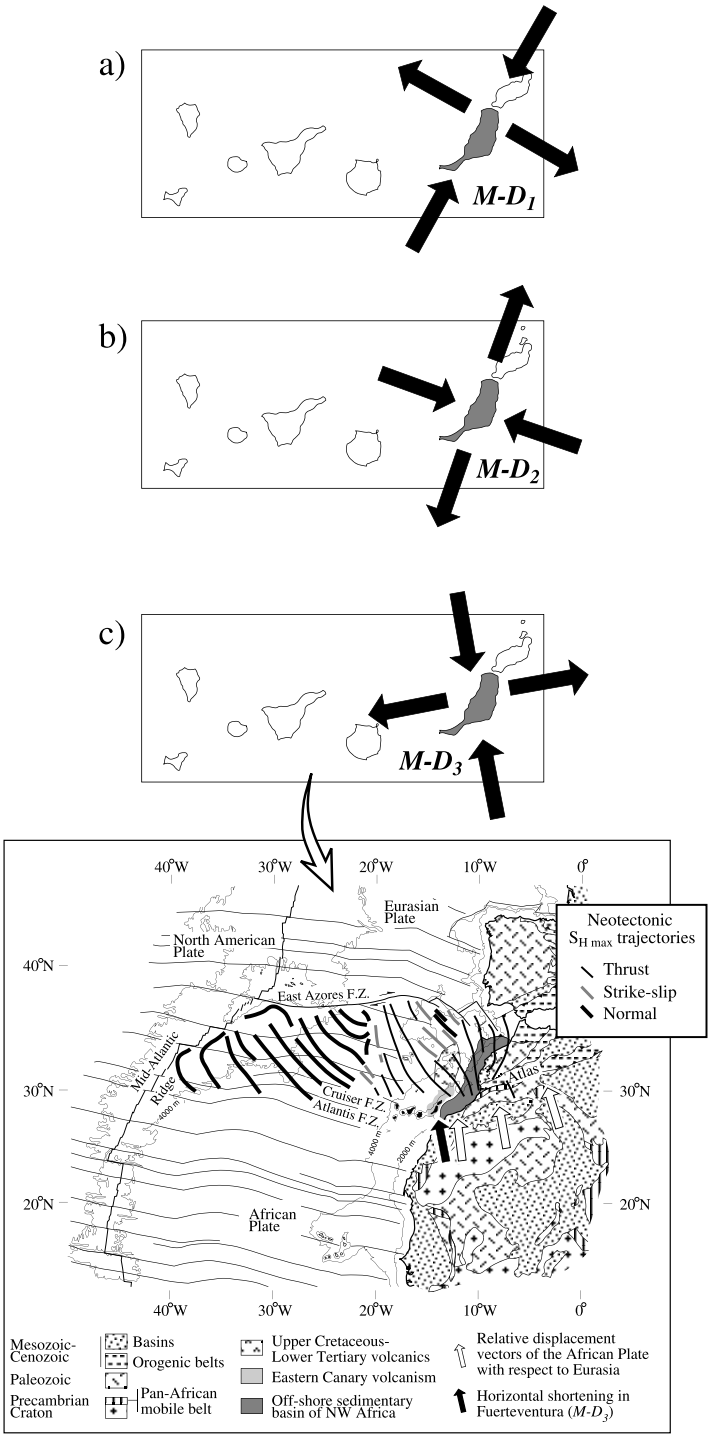

Figure 15. Time evolution of the average deformation fields in Fuerteventura. Black converging arrows: maximum horizontal shortening; black diverging arrows: maximum horizontal extension. (a) M-D_1 phase (25–20 Ma). (b) M-D_2 phase (20–17.2 Ma). (c) M-D_3 phase (17.2–12 Ma); sketch showing the large-scale tectonic framework of the Canary Islands. Patterns of important fracture zones (FZ), bathymetric contours, and plate boundaries are according to *Klitgord and Schouten* [1986] and *Steiner et al.* [1998]; geological features of continental northwestern Africa are after *Guiraud et al.* [1987]; tectonic map of the Atlas system and Iberian Peninsula are modified from *Seber et al.* [1996]; arrows indicating the relative displacement of Africa with respect to Eurasia follow the model of *Argus et al.* [1989]; curves marking the neotectonic stress trajectories and regimes in the NW corner of the African plate are after *Jiménez-Munt and Negredo* [2003].

carded in a model of Miocene asymmetric extension of Fuerteventura.

[40] In summary, it is here proposed that the M-D_1 phase gave place during the early Miocene to an asymmetric extension of the Fuerteventura oceanic lithosphere. The arcuate geometry in plan view of this asymmetric graben recalls the patterns described by *Rosendahl* [1987] in the East Africa Rift. Therefore it is possible to propose a process of Miocene rifting of Fuerteventura. The probable extrapolation of these structures to the north (Lanzarote and Conception Bank, Figure 1), and perhaps to the SW (from the Jandía Peninsula toward the Gran Canaria Island) suggests that this rifting process can be a fundamental characteristic of the eastern Canary ridge (Figure 15a). Magnetic anomalies follow the trend of the eastern Canary ridge, and show a curved, concave northward pattern at the south of Fuerteventura [*Catalán et al.*, 2003], therefore mimicking the arcuate geometry of rifting described in this work.

5.2. Phase M-D_2

[41] The transition to the M-D_2 phase took place at around 20 Ma, and it is marked by the intrusion of plutonic complexes with annular structure [*Ancochea et al.*, 1996]. The faults and dikes assigned to this phase affect the same materials than the M-D_1 phase and most of the Miocene plutonic rocks. It is responsible for the unconformities between episodes CVC-II and CVC-III and between SVC-I and SVC-II. *Feraud* [1981] and *Feraud et al.* [1985] have determined ages ranging from 20 Ma to 17.3 Ma for NW-SE trending dikes (system 2) from the southern part of Fuerteventura. The older SVC-II lava flows have been dated as 17.2 Ma [cf. *Ancochea et al.*, 1996, Table 1]. Accordingly, this phase lasted from 20 Ma to 17.2 Ma (Figure 12), and thus it approximately coincides with phase F_2 of *Ancochea et al.* [1996]. It represents the transition from a predominantly fissural to a central volcanic activity in the Miocene volcanic complexes. In fact, *Ancochea et al.* [1996] described complex dike systems that they have used, among other criteria, to determine the emission centers of the three large volcanic edifices. The radial patterns of dike systems described by *Ancochea et al.* [1996], mostly coincident in age with our systems 2 and 3, geometrically differ from our more constant dike trajectories (Figure 3). As explained before, this is a result of considering the dike trends in the younger episodes of the Miocene volcanic complexes [*Ancochea et al.*, 1996], while in this work we have measured dike data in the basal complex and in the older episodes of the Miocene edifices. More variable dike trends have been observed in the Jandía Peninsula (Figure 10), where radial dike patterns can reflect either volcano spreading or the effect of shallow intrusions exerting magma pressure on their walls and therefore increasing the volcano circumference [e.g., *Odé*, 1957; *Walker*, 1993; *van Wyk de Vries and Merle*, 1996]. However, in the stiff rocks of the basal complex, the subaerial volcanic group and the older units of the Miocene complexes, dike trends are more constant and define regional-scale deformation fields, with minor influence of the overlying edifices, which is indicative of the high viscosity of their substratum, as stated before.

[42] In any case, extension direction changed to NNE-SSW around 20 Myr ago, which is the average trend of the M-D_2 phase (Figures 12 and 15b). To explain this change in the extension direction two hypotheses can be advanced. First, it can be proposed a local switching of deformation axes during the same tectonic phase, a feature observed in the continental crust [e.g., *Simón Gomez*, 1989]. In fact, analysis of the brittle-ductile shear zones that acted during the first stages of the M-D_1 phase indicates a WNW-ESE predominant extension, with a minor extension along the NNE-SSW axis. However, the field structures in Fuerteventura show systematic crosscut relationships, and the trajectories of both deformation fields are not strictly normal (Figure 11). Therefore, in this work a second hypothesis of progressive permutation of deformation axes is favored. This permutation was responsible for a change from a mostly orthogonal rifting (MD-D_1) to an oblique rifting (MD-D_2). Similar tectonic evolutions have been found in many other rift systems, like for instance the Main Ethiopian Rift [*Boccaletti et al.*, 1999].

5.3. Phase M-D_3

[43] Phase MD-D_3 is contemporary with the main stages of growth of the huge volcanic edifices, particularly with respect to the northern volcanic complex (Figures 12 and 14b). It is responsible for the unconformities between episodes SVC-II and SVC-III in the southern volcanic complex and between episodes NVC-I and NVC-II-III in the northern volcanic complex. Dikes of system 3 have yielded ages ranging from 15.4 Ma to 12 Ma in the Jandía Peninsula [*Feraud*, 1981; *Feraud et al.*, 1985]. Therefore MD-D_3 approximately coincides with phase F_3 of *Ancochea et al.* [1996]. The average extension direction is E-W to ENE-WSW (Figure 11). No signs of this phase have been found in the Pliocene and Quaternary sediments and volcanic rocks of Fuerteventura. Therefore phase MD-D_3 can be dated between 17.2 and 12 Ma (Figure 12). Interestingly, the horizontal shortening direction deduced for phase MD-D_3 agrees with that of the present-day relative displacement vector of the African plate with respect to Eurasia in the studied area (Figure 15c) (displacement vectors traced according to the model of *Argus et al.* [1989]). At Lanzarote Island, *Marinoni and Pasquarè* [1994] have identified two strike-slip deformation phases with N-S to WNW-ESE horizontal shortening axes. The age of these events is less than 6 Ma. The orientation of the horizontal deformation axes for these phases in Lanzarote is roughly comparable with that of the MD-D_3 phase of Fuerteventura, and they can represent a time evolution of this phase (from extensional to strike-slip regimes) in the realm of the relative plate motions between Africa and Eurasia. In fact, as stated in the introduction, the theoretical model of *Jiménez-Munt and Negredo* [2003] suggests the present-day predominance of thrust to strike-slip regimes immediately to the north of the Canary Archipelago (Figure 15c), with N-S to NNW-SSE shortening directions. Also the available seismotectonic information for the zone between Gran Canaria and Tenerife, west of

Fuerteventura (Figure 1), supports a NNW-SSE trending maximum horizontal shortening favoring present-day displacement along strike-slip and reverse faults [*Mezcua et al.*, 1992].

5.4. Possible Causes of the Miocene Rifting of Fuerteventura

[44] The relative plate motion between Africa and Eurasia has remained stable since at least 30 Myr to the present [e.g., *Morgan*, 1983; *Roest and Srivastava*, 1991]. Therefore only the orientation of the maximum horizontal shortening associated with the MD-D_3 phase (N-S to NNW-SSE) can be partly explained with the relative plate motions between the African and Eurasian plates, and the origin of the MD-D_1 and MD-D_2 phases must be assigned to more local sources. Rifting and seafloor spreading is a tectonic characteristic of the western Mediterranean region since the Eocene and early Miocene, a paradoxical feature taking into account the colliding tectonic scenario between the African and Eurasian plates. *Hoernle et al.* [1995] suggested that this rifting, and its associated alkaline volcanism, is a consequence of lithosphere uplift above a large region of mantle upwelling. Indeed, *Hoernle et al.* [1995] have shown the presence of a low S wave velocity anomaly beneath the central east Atlantic and the western Mediterranean, depicting a huge sheet-like body. *Teixell et al.* [2005] have discussed the effect in the tectonic evolution of the Atlas Mountains of mantle upwelling in an otherwise contractive setting. The lithosphere thinning (from 180 to 80–60 km) beneath the Atlas could explain its high relief and occurrence of Miocene to recent alkaline magmatism. *Missenard et al.* [2006] proposed that this thermal anomaly can be followed from the Atlas Mountains to the south, across the Atlantic margin, and they relate this thermal anomaly to a shallow mantle plume. According to *Teixell et al.* [2005], mantle upwelling would be associated with upper mantle flow influenced by the thickening of the lithosphere at the Iberia-Africa plate boundary. With respect to the Canary Islands, *Canales and Dañobeitia* [1998] have described a swell rather obscured by the weight of the islands, and probably due to a thermal anomaly ($\sim$360°C) at the base of the lithosphere and upper asthenosphere. Geochemical data show a multicomponent mixture of lithospheric, asthenospheric and deep mantle sources [e.g., *Hoernle et al.*, 1991]. Therefore geophysical and geochemical data support the presence of a sublithospheric thermal anomaly, with mantle upwelling beneath the Canary Islands. The debate over whether this mantle upwelling represents a Miocene to recent plume, remnants of an old, Mesozoic plume, or it is rather a result of large-scale horizontal flow in the upper mantle, is beyond the scope of this work.

[45] Lithosphere uplift and later collapse through the activity of large-scale faults during the MD-D_1 and MD-D_2 phases should have overcome the effect of the deformation field related to the Africa-Eurasia relative convergent displacement. The end of phase MD-D_3 coincides with the waning of the volcanic activity in Fuerteventura. It is possible to relate this feature to the increasing relative importance of the deformation fields associated with the African plate kinematics. The mantle anomaly was almost exhausted beneath Fuerteventura by the end of the middle Miocene, thus decreasing the importance of the local versus plate-scale strain fields. This transition corresponds to the switching between the extensional regime of phase MD-D_3 and the strike-slip regimes prevailing in more recent times, always with a N-S to NNW-SSE trending axis of maximum horizontal shortening. Interestingly, E-W trending extension still predominated until around 1.2 Ma in La Palma (location in Figure 1) [*Fernández et al.*, 2002]. This suggests that the transition from local to plate-scale strain fields probably suffered a westward migration with time, from the eastern Canary ridge (more than 6 Ma and less than 12 Ma in Fuerteventura and Lanzarote) toward the western Canary Islands (less than 1.2 Ma in La Palma). Similar age variations have been cited for the history of the subaerial volcanic activity in the Canaries [e.g., *Ancochea*, 2004].

[46] The evolution from phases MD-D_1 to MD-D_2, and then to MD-D_3, is characterized by the change from fissural volcanic activity toward predominantly central volcanic emissions. The model suggested by *Walter et al.* [2005] to explain the evolution of the Anaga volcano on the island of Tenerife (location in Figure 1) can also be applied to the Fuerteventura example. The model of *Walter et al.* [2005] considers the evolution of a linear rift that suffers local reorganization through flank instability and consequent generation of giant landslides. As a result of the variation in geometry and stress field triggered by the landslides, the linear rift evolves to triple-armed rifts that focus volcanic emissions on central edifices. *Walter et al.* [2005] have tested the model with a numerical elastic dislocation model. Giant landslides dominated the episodic growth of the volcanic edifices of Fuerteventura [*Ancochea et al.*, 1996; *Stillman*, 1999; *Acosta et al.*, 2003]. This instability can be partly explained by the syntectonic evolution of these volcanic edifices. Therefore it seems possible to apply the model of rift zone reorganization to the Miocene volcanic evolution of Fuerteventura. Apart from the possible mechanical effects of large landslides, tectonic switching from NW-SE to NNE-SSW and then to ENE-WSW extension directions should have collaborated in the construction of large central edifices. During the MD-D_2 and MD-D_3 phases the magmas could have profited the intersections between fractures resulting from the distinct tectonic events, such that ascent conduits could have taken a vertical elongate shape (Figure 14b). In this sense, the center of the northern edifice (Figure 1 for location) coincides with the inland prolongation of NW-SE faults observed in the west coast (Figure 7a) and that can be assigned to phase M-D_2. The age differences in the construction of the three large edifices in Fuerteventura are probably a consequence of local structural patterns and local evolution of volcanic emission and flank instabilities. The center of the older edifice (the CVC, Figure 12) coincides with the central segment of the sigmoid extensional structure (Figure 14b), probably the most mature part of the fault system that shows the larger extension factor.

[47] The complex image that emerges from this study can be used to constrain the models proposed for the origin

of the Canary Islands. The long and changing tectonic history of Fuerteventura, with a long-living rifting activity, is more akin to the unifying model of *Anguita and Hernán* [2000], which integrates the thermal and mechanical history and properties of the lithosphere and the sublithospheric mantle, than to any of the single hypotheses described in section 1.

6. Conclusions

[48] Three Miocene extensional deformation phases ($M\text{-}D_1$, $M\text{-}D_2$, and $M\text{-}D_3$) are recognized in the Fuerteventura Island. $M\text{-}D_1$ is characterized by a NW-SE directed extension. This phase, which lasted from 25 to 20 Ma, probably generated a large asymmetrical fault system, with predominantly top-to-NW sense of displacement. Syntectonic with this phase were the emplacement of a dense dike swarm, and the deposition of several volcanic units. Volcanic activity was essentially fissural during this stage. Folding of the pretectonic and syntectonic successions is interpreted as due to the accommodation of these series to complex ramp/flat geometry in the hypothetical basal detachment. The extensional structures are sigmoid in plan view, recalling the arcuate geometry of grabens in some continental rift systems. A switching to NNE-SSW extension directions took place during phase $M\text{-}D_2$ (20–17.2 Ma). This phase is contemporary to the inception of the large central volcanic edifices in Fuerteventura. This change in the extension directions is believed to have conditioned the transition from fissural to central volcanic emission types. Finally, phase $M\text{-}D_3$ (17.2–12 Ma) was characterized by ENE-WSW extension or NNW-SSE shortening, which coincides with the displacement trajectories predicted by plate tectonic models in this part of the African plate. The Miocene rifting of Fuerteventura is considered as the tectonic result of the upwelling of a large body of anomalous sublithosphere mantle, which exceeded the deformation associated with plate motions, and generated a voluminous, tectonically controlled, basic volcanism. This evolution is akin to that of the Atlas province during the same time period, and it should be taken into account in any model for the origin of the Canary Islands.

[49] **Acknowledgments.** Financial support from project BTE2003-00569 of the Spanish Ministry of Education and Science and project PI2003/106 of the Canary Government is gratefully acknowledged. C.F., E.G.N., and M.A.C. also acknowledge support from the Junta de Andalucía (RNM-316) and the Universidad de Huelva (Plan Propio de Investigación). Detailed reviews by Valerio Acocella, John Walsh, and an anonymous referee considerably improved the original manuscript and are gratefully acknowledged. We also thank the Cabildo Insular de Fuerteventura and the Spanish Ejército de Tierra (RIL Soria) for their help during the field work.

References

Acosta, J., E. Uchupi, A. Muñoz, P. Herranz, C. Palomo, M. Ballesteros, and ZEE Working Group (2003), Geologic evolution of the Canarian Islands of Lanzarote, Fuerteventura, Gran Canaria and La Gomera and comparison of landslides at these islands with those at Tenerife, La Palma and El Hierro, *Mar. Geophys. Res.*, *24*, 1–40.

Ahijado, A. (1999), Las intrusiones plutónicas e hipoabisales del sector meridional del Complejo Basal de Fuerteventura, Ph.D. thesis, 392 pp., Univ. Complutense de Madrid, Madrid, Spain.

Ahijado, A., and A. Hernández-Pacheco (1990), Las rocas ultramáficas alcalinas del Jable de Salinas, Fuerteventura, Islas Canarias, *Rev. Soc. Geol. Esp.*, *3*, 275–287.

Ahijado, A., R. Casillas, and A. Hernández-Pacheco (2001), The dike swarms of the Amanay Massif, Fuerteventura, Canary Islands, *J. Asian Earth Sci.*, *19*, 333–345.

Allerton, S., and F. J. Vine (1987), Spreading structure of the Troodos ophiolite, Cyprus: Some paleomagnetic constraints, *Geology*, *15*, 593–597.

Ancochea, E. (2004), Canarias: Evolución de la actividad volcánica, in *Geología de España*, edited by J. A. Vera, pp. 639–641, Inst. Geol. y Minero de Esp.-Soc. Geol. de Esp., Madrid.

Ancochea, E., J. L. Brandle, C. R. Cubas, F. Hernán, and M. J. Huertas (1993), La Serie I de la Isla de Fuerteventura, *Mem. R. Acad. Cien. Ex. Fis. Nat.*, *27*, 151 pp.

Ancochea, E., J. L. Brandle, C. R. Cubas, F. Hernán, and M. J. Huertas (1996), Volcanic complexes in the eastern ridge of the Canary Islands: The Miocene activity of the Island of Fuerteventura, *J. Volcanol. Geotherm. Res.*, *70*, 183–204.

Anguita, F., and F. Hernán (1975), A propagating fracture model versus a hot-spot origin for the Canary Islands, *Earth Planet. Sci. Lett.*, *27*, 11–19.

Anguita, F., and F. Hernán (2000), The Canary Islands origin: A unifying model, *J. Volcanol. Geotherm. Res.*, *103*, 1–26.

Araña, V., and R. Ortiz (1991), The Canary Islands: Tectonics, magmatism and geodynamic framework, in *Magmatism in Extensional Structural Settings—The Phanerozoic Agrican Plate*, edited by A. B. Kampunzu and R. T. Lubala, pp. 209–249, Springer, New York.

Argus, D. F., R. G. Gordon, C. DeMets, and S. Stein (1989), Closure of the Africa-Eurasia-North America plate motion circuit and tectonics of the Gloria fault, *J. Geophys. Res.*, *94*, 5585–5602.

Balcells, R., J. L. Barrera, J. A. Gómez, L. A. Cueto, E. Ancochea, M. J. Huertas, E. Ibarrola, and N. Snelling (1994), Edades radiométricas de los edificios miocenos de Fuerteventura (Islas Canarias), *Bol. Geol. Minero*, *105*, 50–56.

Balogh, K., A. Ahijado, R. Casillas, and C. Fernández (1999), Contributions to the chronology of the Basal Complex of Fuerteventura, Canary Islands, *J. Volcanol. Geotherm. Res.*, *90*, 81–102.

Banda, E., J. J. Dañobeitia, E. Suriñach, and J. Ansorge (1981), Features of crustal structure under the Canary Islands, *Earth Planet. Sci. Lett.*, *55*, 11–24.

Boccaletti, M., R. Mazzuoli, M. Bononi, T. Trua, and B. Abebe (1999), Plio-Quaternary volcanotectonic activity in the northern sector of the Main Ethiopian Rift: Relationships with oblique rifting, *J. Afr. Earth Sci.*, *29*, 679–698.

Bull, J. M., T. A. Minshull, N. C. Mitchell, K. Thors, J. K. Dix, and A. I. Best (2003), Fault and magmatic interaction within Iceland's western rift over the last 9 kyr, *Geophys. J. Int.*, *154*, F1–F8.

Canales, J. P., and J. Dañobeitia (1998), The Canary Islands swell: A coherence analysis of bathymetry and gravity, *Geophys. J. Int.*, *132*, 479–488.

Cantagrel, J. M., J. M. Fúster, C. Pin, U. Renaud, and E. Ibarrola (1993), Age Miocène inférieur des carbonatites de Fuerteventura, *C. R. Acad. Sci.*, *316*, 1147–1153.

Carracedo, J. C., S. Day, H. Guillou, E. Rodríguez, J. A. Canas, and F. J. Pérez (1998), Hotspot volcanism close to a passive continental margin, *Geol. Mag.*, *135*, 591–604.

Casillas, R., A. Ahijado, and A. Hernández-Pacheco (1994), Zonas de cizalla dúctil en el complejo basal de Fuerteventura, *Geogaceta*, *15*, 117–120.

Catalán, M., J. Martín Dávila, and ZEE Working Group (2003), A magnetic anomaly study offshore the Canary Archipelago, *Mar. Geophys. Res.*, *24*, 129–148.

Cecchi, E., B. van Wyk de Vries, and J. M. Lavest (2005), Flank spreading and collapse of weak-cored volcanoes, *Bull. Volcanol.*, *67*, 72–91.

Coello, J., J. M. Cantagrel, F. Hernán, J. M. Fúster, E. Ibarrola, E. Ancochea, C. Casquet, J. R. Jamond, and A. Cendrero (1992), Evolution of the eastern volcanic ridge of the Canary Islands based on new K-Ar data, *J. Volcanol. Geotherm. Res.*, *53*, 251–274.

Dañobeitia, J. J. (1988), Reconocimiento geofísico de estructuras submarinas situadas al norte y sur del Archipiélago Canario, *Rev. Soc. Geol. Esp.*, *1*, 143–155.

Dañobeitia, J. J., and J. O. Canales (2000), Magmatic underplating in the Canary Archipelago, *J. Volcanol. Geotherm. Res.*, *103*, 27–41.

Feraud, G. (1981), Datation de resseaux de dykes et de roches volcaniques sous-marines par le methods K-Ar et ^{40}Ar-^{39}Ar: Utillisation des dykes comme marqueur de paleoconstraintes, Ph.D. thesis, 130 pp., Univ. de Nice, Nice, France.

Feraud, G., G. Giannérini, R. Campredon, and C. J. Stillman (1985), Geochronology of some Canarian dike swarms: Contribution to the volcano-tectonic evolution of the Archipielago, *J. Volcanol. Geotherm. Res.*, *25*, 29–52.

Fernández, C., R. Casillas, A. Ahijado, V. Perelló, and A. Hernández-Pacheco (1997), Shear zones as result of intraplate tectonics in oceanic crust: An example of the Basal Complex of Fuerteventura (Canary Islands), *J. Struct. Geol.*, *19*, 41–57.

Fernández, C., J. De la Nuez, R. Casillas, and E. García (2002), Stress fields associated with the growth of a large shield volcano (La Palma, Canary Islands), *Tectonics*, *21*(4), 1031, doi:10.1029/2000TC900038.

Foulger, G. R., J. H. Natland, D. C. Presnall, and D. L. Anderson (Eds.) (2005), *Plates, Plumes and Paradigms*, *Spec. Pap. Geol. Soc. Am.*, *388*, 861 pp.

Fúster, J. M. (1975), Las Islas Canarias: Un ejemplo de evolución temporal y espacial del vulcanismo oceánico, *Estud. Geol.*, *31*, 439–463.

Fúster, J. M., A. Cendrero, P. Gastesi, E. Ibarrola, and J. Lopez Ruiz (1968), *Geología y volcanología de las Islas Canarias–Fuerteventura*, Instituto ''Lucas Mallada'', Consejo Superior de Invest. Cient., Madrid.

Fúster, J. M., M. Muñoz, J. Sagredo, A. Yébenes, T. Bravo, and A. Hernández-Pacheco (1980), Excursión n° 121 A + c del 26° I.G.C. a las Islas Canarias, *Bol. Inst. Geol. Min. Esp.:*, *92*, 351–390.

Fúster, J. M., J. L. Barrera, M. Muñoz, J. Sagredo, and A. Yébenes (1984a), Mapa y Memoria explicativa de la Hoja de Pájara (1106 IV) del mapa geológico nacional a escala 1:25.000, Inst. Geol. y Minero de Esp., Madrid.

Fúster, J. M., A. Yébenes, J. L. Barrera, M. Muñoz, and J. Sagredo (1984b), Mapa y Memoria explicativa de la Hoja de Betancuria (1106 II) del mapa geológico nacional a escala 1:25.000, Inst. Geol. y Minero de Esp., Madrid.

Gastesi, P. (1969), Petrology of the ultramafic and basic rocks of Betancuria massif, Fuerteventura Island (Canarian Archipelago), *Bull. Volcanol.*, *33*, 1008–1038.

Gibbs, A. D. (1983), Balanced cross-section construction from seismic sections in areas of extensional tectonics, *J. Struct. Geol.*, *5*, 153–160.

Guiraud, R., Y. Bellion, J. Benkhelil, and C. Moreau (1987), Post-Hercynian tectonics in northern and western Africa, *Geol. J.*, *22*, 433–466.

Gutiérrez, M. (2000), Estudio petrológico, geoquímico y estructural de la serie volcánica submarina del Complejo Basal de Fuerteventura (Islas Canarias): Caracterización del crecimiento submarino y de la emersión de la Isla, Ph.D. thesis, 533 pp., Univ. de La Laguna, La Laguna, Spain.

Gutiérrez, M., R. Casillas, C. Fernández, K. Balogh, A. Ahijado, C. Castillo, J. R. Colmenero, and E. García-Navarro (2006), The submarine volcanic succession of the Basal Complex of Fuerteventura, Canary Islands: A model of submarine growth and emersion of some tectonic volcanic islands, *Geol. Soc. Am. Bull.*, *118*, 785–804.

Hobson, A., F. Bussy, and J. Hernández (1998), Shallow-level migmatization of gabbros in a metamorphic contact aureole, Fuerteventura Basal Complex, Canary Islands, *J. Petrol.*, *39*, 125–137.

Hoernle, K., and H. U. Schmincke (1993), The role of partial melting in the 15–Ma geochemical evolution of Gran Canaria: A blob model for the Canary hotspot, *J. Petrol.*, *34*, 599–626.

Hoernle, K., G. Tilton, and H. W. Schmincke (1991), Sr-Nd-Pb isotopic evolution of Gran Canaria: Evidence for shallow enriched mantle beneath the Canary Islands, *Earth Planet. Sci. Lett.*, *106*, 44–63.

Hoernle, K., Y. S. Zhang, and D. Graham (1995), Seismic and geochemical evidence of large-scale mantle upwelling beneath the eastern Atlantic and western and central Europe, *Nature*, *374*, 34–39.

Holik, J. S., P. D. Rabinowitz, and J. A. Austin (1991), Effects of the Canary hotspot volcanism on structure of oceanic crust off Morocco, *J. Geophys. Res.*, *96*, 12,039–12,067.

Homberg, C., J. Angelier, F. Bergerat, and O. Lacombe (2004), Using stress deflections to identify slip events in fault systems, *Earth Planet. Sci. Lett.*, *2217*, 409–424.

Ibarrola, E., J. M. Fúster, and J. M. Cantagrel (1989), Edades K-Ar de las rocas volcánicas submarinas del sector norte del Complejo Basal de Fuerteventura, paper presented at ESF Meeting on Canarian Volcanism, Eur. Sci. Found., Lanzarote, Spain.

Jackson, M. D., and D. D. Pollard (1990), Flexure and faulting of sedimentary host rocks during growth of igneous domes, Henry Mountains, Utah, *J. Struct. Geol.*, *12*, 185–206.

Javoy, M., C. J. Stillman, and C. Pineau (1986), Oxygen and hydrogen isotope studies on the basal complexes of the Canary Islands: Implications on the conditions of their genesis, *Contrib. Mineral. Petrol.*, *92*, 225–235.

Jiménez-Munt, I., and A. M. Negredo (2003), Neotectonic modelling of the western part of the Africa-Eurasia plate boundary: From the Mid-Atlantic Ridge to Algeria, *Earth Planet. Sci. Lett.*, *205*, 257–271.

Kamb, W. B. (1959), Ice petrofabric observations from Blue Glacier, Washington, in relation to theory and experiment, *J. Geophys. Res.*, *64*, 1891–1909.

Klitgord, K. D., and H. Schouten (1986), Plate kinematics of the central Atlantic, in *The Geology of North America*, vol. M, *The Western North Atlantic Region*, edited by P. R. Vogt and B. E. Tucholke, pp. 351–378, Geol. Soc. of Am., Boulder, Colo.

Lawn, B. R., and T. R. Wilshaw (1975), *Fracture of Brittle Solids*, Cambridge Univ. Press, New York.

Le Bas, M. J., D. C. Rex, and C. J. Stillman (1986), The early magmatic chronology of Fuerteventura, *Geol. Mag.*, *123*, 287–298.

Lee, C., and J. Angelier (1994), Paleostress trajectory maps based on the results of local determinations: The ''LISSAGE'' program, *Comput. Geosci.*, *20*, 161–191.

López Ruiz, L. (1970), Estudio petrográfico y geoquímico del Complejo filoniano de Fuerteventura (Islas Canarias), *Estud. Geol.*, *26*, 173–208.

Mardia, K. V. (1972), *Statistics of Directional Data*, Elsevier, New York.

Marinoni, L. B. (2001), Crustal extension from exposed sheet intrusions: Review and method proposal, *J. Volcanol. Geotherm. Res.*, *107*, 27–46.

Marinoni, L. B., and A. Gudmundsson (2000), Dykes, faults and palaeostresses in the Teno and Anaga massifs of Tenerife (Canary Islands), *J. Volcanol. Geotherm. Res.*, *103*, 83–103.

Marinoni, L. B., and G. Pasquarè (1994), Tectonic evolution of the emergent part of a volcanic ocean island: Lanzarote, Canary Islands, *Tectonophysics*, *239*, 111–135.

Marret, R., and R. W. Allmendinger (1990), Kinematic analysis of fault-slip data, *J. Struct. Geol.*, *12*, 973–986.

McClay, K. R., and A. D. Scott (1991), Experimental models of hangingwall deformation in ramp-flat listric extensional fault systems, *Tectonophysics*, *188*, 85–96.

McGuire, W. J., , A. P. Jones, and J. Neuberg (Eds.) (1996), *Volcano Instability on the Earth and Other Planets*, *Geol. Soc. Spec. Publ.*, *110*, 388 pp.

McPhie, J., M. Doyle, and R. Allen (1993), *Volcanic Textures: A Guide to the Interpretation of Textures in Volcanic Rocks*, 1st ed., 198 pp., Center for Ore Deposit and Explor. Stud., Univ. of Tasmania, Tasmanian Govt. Print. Off., Hobart.

Meco, J., and R. S. Pomel (1985), Les formaciones marines et continentales intervolcaniques des Iles Canaries Orientales (Grande Canarie, Fuerteventura et Lanzarote), stratigraphie et signification paleoclimatique, *Estud. Geol.*, *41*, 223–227.

Meco, J., and C. E. Stearns (1981), Emergent littoral deposits in the Eastern Canary Islands, *Quat. Res.*, *15*, 199–208.

Merle, O., and A. Borgia (1996), Scaled experiments of volcanic spreading, *J. Geophys. Res.*, *101*, 13,805–13,817.

Mezcua, J., E. Buforn, A. Udías, and J. Rueda (1992), Seismotectonics of the Canary Islands, *Tectonophysics*, *208*, 447–452.

Missenard, Y., H. Zeyen, D. Frizon de Lamotte, P. Leturmy, C. Petit, M. Sébrier, and O. Saddiqi (2006), Crustal versus asthenospheric origin of relief of the Atlas Mountains of Morocco, *J. Geophys. Res.*, *111*, B03401, doi:10.1029/2005JB003708.

Morgan, W. J. (1971), Convection plumes in the lower mantle, *Nature*, *230*, 42–43.

Morgan, W. J. (1983), Hotspot tracks and the early rifting of the Atlantic, *Tectonophysics*, *94*, 123–139.

Muñoz, M. (1969), Estudio petrológico de las formaciones alcalinas de Fuerteventura (Islas Canarias), *Estud. Geol.*, *25*, 257–310.

Muñoz, M., and J. Sagredo (1994), Reajustes mineralógicos y geoquímicos producidos durante el metamorfismo de contacto de diques basálticos (Fuerteventura, Islas Canarias), *Bol. Soc. Esp. Min.*, *17*, 86–87.

Muñoz, M., J. Sagredo, P. J. Rincón-Calero, and R. Vegas (1997), Emplazamiento en una zona de cizalla dúctil-frágil transtensiva para el plutón de Pájara, Fuerteventura, Islas Canarias, *Geogaceta*, *21*, 171–174.

Muñoz, M., J. Sagredo, C. de Ignacio, J. Fernández-Suárez, and T. E. Jeffries (2005), New data (U-Pb, K-Ar) on the geochronology of the alkaline-carbonatitic association of Fuerteventura, Canary Islands, Spain, *Lithos*, *85*, 140–153.

Odé, H. (1957), Mechanical analysis of the dyke pattern of the Spanish Peaks area, Colorado, *Geol. Soc. Am. Bull.*, *68*, 567–576.

Oehler, J. F., B. van Wyk de Vries, and P. Labazuy (2005), Landslides and spreading of oceanic hotspot and arc shield volcanoes on low strength layers (LSLs): An analogue modeling approach, *J. Volcanol. Geotherm. Res.*, *144*, 169–189.

Pollard, D. D., and P. Segall (1987), Theoretical displacements and stresses near fractures in rock: With applications to fault, joints, veins, dikes, and solution surface, in *Fracture Mechanism of Rocks*, edited by B. K. Attkinson, pp. 227–349, Elsevier, New York.

Robertson, A. H. F., and D. Bernouilli (1982), Stratigraphy, facies and significance of Late Mesozoic and early Tertiary sedimentary rocks of Fuerteventura (Canary Islands) and Maio (Cape Verde Islans), in *Geology of the Northwest African Continental Margin*, edited by U. Von Rad et al., pp. 498–525, Springer, New York.

Robertson, A. H. F., and C. J. Stillman (1979a), Late Mesozoic sedimentary rocks of Fuerteventura, Canary Islands. Implications for West Africa continental margin evolution, *J. Geol. Soc. London*, *36*, 47–60.

Robertson, A. H. F., and C. J. Stillman (1979b), Submarine volcanic and associated sedimentary rocks of the Fuerteventura Basal Complex, Canary Islands, *Geol. Mag.*, *116*, 203–214.

Roest, W. R., and S. P. Srivastava (1991), Kinematics of the plate boundaries between Eurasia, Iberia, and Africa in the North Atlantic from the Late Cretaceous to the present, *Geology*, *19*, 613–616.

Rosendahl, B. R. (1987), Architecture of continental rifts with special reference to East Africa, *Annu. Rev. Earth Planet. Sci.*, *15*, 445–503.

Sagredo, J., E. Ancochea, J. L. Brändle, C. R. Cubas, J. M. Fúster, A. Hernández-Pacheco, and M. Muñoz (1989), Magmatismo hipoabisal-subvolcánico y vulcanismo en un ámbito geodinámico distensivo (Fuerteventura, Islas Canarias), paper presented at ESF Meeting on Canarian volcanism, Eur. Sci. Found., Lanzarote, Canary Islands, Spain.

Sagredo, J., M. Muñoz, and C. Galindo (1996), Características petrológicas y edad K-Ar de las sienitas nefelínicas del Morro del Recogedero (Fuerteventura, Islas Canarias), *Geogaceta*, *20*, 506–509.

Scheidegger, A. E. (1965), On the statistics of the orientation of bedding planes, grain axes and similar sedimentological data, *U.S. Geol. Surv. Prof. Pap.*, *525C*, 164–167.

Searle, R. (1980), Tectonic pattern of the Azores spreading centre and triple junction, *Earth Planet. Sci. Lett.*, *51*, 415–434.

Seber, D., M. Barazangi, B. A. Tadili, M. Ramdani, A. Ibenbrahim, and D. Ben Sari (1996), Three-dimensional upper mantle structure beneath the intraplate Atlas and interplate Rif mountains of Morocco, *J. Geophys. Res.*, *101*, 3125–3138.

Simón Gomez, J. L. (1989), Late Cenozoic stress field and fracturing in the Iberian Chain and Ebro Basin (Spain), *J. Struct. Geol.*, *11*, 285–294.

Steiner, C., A. Hobson, P. Favre, and G. M. Stampli (1998), Early Jurassic sea-floor spreading in the central Atlantic -the Jurassic sequence of Fuerteventura (Canary Islands), *Geol. Soc. Am. Bull.*, *110*, 1304–1317.

Stillman, C. J. (1987), A Canary Islands dyke swarm: Implications for the formation of oceanic islands by extensional fissural volcanism, in *Mafic Dyke Swarms*, edited by H. C. Halls and W. F. Fahrig, *Spec. Pap. Geol. Assoc. Can.*, *34*, 243–255.

Stillman, C. J. (1999), Giant Miocene landslides and the evolution of Fuerteventura, Canary Islands, *J. Volcanol. Geotherm. Res.*, *94*, 89–104.

Stillman, C. J., and A. H. F. Robertson (1977), The dyke swarm of the Fuerteventura Basal Complex, Canary Islands, *Abstr. Geol. Soc. London Newslett.*, *6*, 8.

Stillman, C. J., J. M. Fuster, M. J. Bennell-Baker, M. Muñoz, J. D. Smewing, and J. Sagredo (1975), Basal Complex of Fuerteventura (Canary Islands) is an oceanic intrusive complex with rift-system affinities, *Nature*, *257*, 469–471.

Teixell, A., P. Ayarza, H. Zeyen, M. Fernàndez, and M. L. Arboleya (2005), Effects of mantle upwelling in a compressional setting: The Atlas Mountains of Morocco, *Terra Nova*, *17*, 456–461.

van Wyk de Vries, B., and R. Matela (1998), Styles of volcano-induced deformation: Numerical models of substratum flexure, spreading and extrusion, *J. Volcanol. Geotherm. Res.*, *81*, 1–18.

van Wyk de Vries, B., and O. Merle (1996), The effect of volcanic constructs on rift fault patterns, *Geology*, *24*, 643–646.

van Wyk de Vries, B., S. Self, P. W. Francis, and L. Keszthelyi (2001), A gravitational spreading origin for the Socompa debris avalanche, *J. Volcanol. Geotherm. Res.*, *105*, 225–247.

Walker, G. P. L. (1987), The dike complex of Koolau volcano, Oahu: Internal structure of a Hawaiian rift zone, *U.S. Geol. Surv. Prof. Pap.*, *1350*, 961–993.

Walker, G. P. L. (1993), Basaltic-volcano systems, in *Magmatic Processes and Plate Tectonics*, edited by H. M. Prichard et al., *Geol. Soc. Spec. Publ.*, *76*, 3–38.

Walter, T. R., V. R. Troll, B. Cailleau, A. Belousov, H. U. Schmincke, F. Amelung, and P. v. d. Bogaard (2005), Rift zone reorganization through flank instability in ocean island volcanoes: An example from Tenerife, Canary Islands, *Bull. Volcanol.*, *67*, 281–291.

Watts, A. B. (1994), Crustal structure, gravity anomalies and flexure of the lithosphere in the vicinity of the Canary Islands, *Geophys. J.*, *119*, 648–666.

Weigel, W., P. Goldflam, and K. Hinz (1978), The crustal structure of the Conception Bank, *Mar. Geophys. Res.*, *3*, 381–392.

Williams, G., and I. Vann (1987), The geometry of listric normal faults and deformation in their hangingwalls, *J. Struct. Geol.*, *9*, 789–795.

Wooller, L., B. van Wyk de Vries, J. B. Murray, H. Rymer, and S. Meyer (2004), Volcano spreading controlled by dipping substrata, *Geology*, *32*, 573–576.

Zazo, C., J. L. Goy, C. Hillaire-Marcell, P. Y. Gillot, V. Soler, J. A. González, C. J. Dabrio, and B. Ghaleb (2002), Raised marine sequences of Lanzarote and Fuerteventura revisited: A reappraisal of relative sea-level changes and vertical movements in the eastern Canary Islands during the Quaternary, *Quat. Sci. Rev.*, *21*, 2019–2046.

A. Ahijado and R. Casillas, Departamento de Edafología y Geología, Universidad de La Laguna, 38206-La Laguna, Tenerife, Canary Islands, Spain.

M. A. Camacho, C. Fernández, and E. García Navarro, Departamento de Geodinámica y Paleontología, Universidad de Huelva, E-21071 Huelva, Spain. (fcarlos@uhu.es)

M. Gutiérrez, Estudios del Terreno S.L., C/España 21, locales 13 y 14, 38390-Santa Úrsula, Santa Cruz de Tenerife, Canary Islands, Spain.